L'Institut Agro Rennes-Angers
☐ **Site d'Angers** ☒ **Site de Rennes**

Année universitaire : 2024 - 2025 Spécialité : Ingénieur agronome Spécialisation (et option éventuelle) : Sciences Halieutiques et Aquacoles	**Mémoire de fin d'études** ☒ d'ingénieur de l'Institut Agro Rennes-Angers (Institut national d'enseignement supérieur pour l'agriculture, l'alimentation et l'environnement) ☐ de master de l'Institut Agro Rennes-Angers (Institut national d'enseignement supérieur pour l'agriculture, l'alimentation et l'environnement) ☐ de l'Institut Agro Montpellier (étudiant arrivé en M2) ☐ d'un autre établissement (étudiant arrivé en M2)

A seasonal population dynamics model to understand intra-annual variability in sardine demographic processes in the Bay of Biscay

Par : Mila DERU

Soutenu à Rennes le 10/09/2025

Devant le jury composé de :

Président : Pablo Brosset

Maître de stage : Maxime Olmos

Enseignant référent : Pablo Brosset

Autres membres du jury (Nom, Qualité) :

Etienne Rivot, Enseignant-Chercheur en écologie halieutique, Institut Agro Rennes

Mathieu Doray, Chercheur en écologie halieutique, Ifremer Nantes

Les analyses et les conclusions de ce travail d'étudiant n'engagent que la responsabilité de son auteur et non celle de l'Institut Agro Rennes-Angers

Annexe III : Fiche de confidentialité et de diffusion du mémoire

Confidentialité

☒ Non ☐ Oui si oui : ☐ 1 an ☐ 5 ans ☐ 10 ans

Pendant toute la durée de confidentialité, aucune diffusion du mémoire n'est possible [1].

Date et signature du **maître de stage** [2] :
(ou de l'étudiant-entrepreneur)

A la fin de la période de confidentialité, sa diffusion est soumise aux règles ci-dessous (droits d'auteur et autorisation de diffusion par l'enseignant à renseigner).

Droits d'auteur

L'auteur[3] Nom Prénom Déru Mila

autorise la diffusion de son travail (immédiatement ou à la fin de la période de confidentialité)

☒ Oui ☐ Non

Si oui, il autorise

☐ la diffusion papier du mémoire uniquement(4)

☐ la diffusion papier du mémoire et la diffusion électronique du résumé

☒ la diffusion papier et électronique du mémoire (joindre dans ce cas la fiche de conformité du mémoire numérique et le contrat de diffusion)

(Facultatif) ☐ accepte de placer son mémoire sous licence Creative commons CC-By-Nc-Nd (voir Guide du mémoire Chap 1.4 page 6)

Date et signature de l'auteur : le 09/09/2025

Autorisation de diffusion par le responsable de spécialisation ou son représentant

L'enseignant juge le mémoire de qualité suffisante pour être diffusé (immédiatement ou à la fin de la période de confidentialité)

☒ Oui ☐ Non

Si non, seul le titre du mémoire apparaîtra dans les bases de données.

Si oui, il autorise

☐ la diffusion papier du mémoire uniquement(4)

☐ la diffusion papier du mémoire et la diffusion électronique du résumé

☒ la diffusion papier et électronique du mémoire

Date et signature de l'enseignant :

27/10/2025

(1) L'administration, les enseignants et les différents services de documentation de l'Institut Agro Rennes-Angers s'engagent à respecter cette confidentialité.
(2) Signature et cachet de l'organisme
(3) Auteur = étudiant qui réalise son mémoire de fin d'études
(4) La référence bibliographique (= Nom de l'auteur, titre du mémoire, année de soutenance, diplôme, spécialité et spécialisation/Option)) sera signalée dans les bases de données documentaires sans le résumé

Annexe III bis

Avant-propos

Utilisation d'une Intelligence Artificielle générative (IAg) pour la rédaction du mémoire

Des outils d'intelligence artificielle générative ont-ils été utilisés ?

☐ Non ☒ Oui

Si oui, préciser pour quels usages :

Correction et reformulatic

Acknowledgments

First, I would like to sincerely thank my tutor, Maxime Olmos, for his availability and guidance throughout this internship and my PhD search. I have learned so much and feel more confident about my future work.

I am also grateful to Guillermo Boyra, in charge of the JUVENA survey, for providing access to the data used in this work.

I would like to thank everyone on the LBH team for making my stay at Ifremer both friendly and enjoyable. Thank you to Paul for your valuable insights on my work, and to Christophe for your precious advice and your jokes. Of course, thank you to Raphaëlle, Klervi, Emma and Eleni for the moments shared in and out of work, as well as my dear office mates, Mathilde and Martin.

Thanks also to my friends in Brest—Ambre, Simon, Aude, and Clément—who made my weekends bright, even in this often grey city.

Finally, I want to express my gratitude to the PELGAS 2025 team, who made this experience even better than I could have imagined!

Contents

List of Figures

List of Tables

List of Appendices

1. Introduction

An important challenge in population ecology is to unravel the mechanisms underlying changes in population dynamics. Understanding patterns in terms of the demographic processes that produce those changes is required to provide reliable conservation and management advice (Schaub and Abadi, 2011). However, shedding light on these mechanisms requires reflecting on the notion of scale in ecology (Levin, 1992; Levin et al., 1997). A mismatch between the scale of the study and the scale of the relevant ecological processes can lead to an inability to identify the ecological and demographic processes driving the population dynamics (Allen et al., 1992), and then to bias in estimated quantities for management and conservation.

When considering temporal scale, seasonality is an important feature as it represents the regular and periodic changes in a state within a year and is driven by periodic climatic condition (White and Hastings, 2020; Williams et al., 2017). In population dynamics, seasonality determines many demographic processes, such as reproduction (Olmos et al., 2023), growth (Merritt et al., 2001) and survival (Rockwell et al., 2017). To complete their life cycle, animals face an annual cycle of productive and unproductive periods. These inter- and intra-annual cycles, along with other seasonal variations in abiotic factors and associated biotic interactions, shape the dynamics of wild animal populations (Varpe, 2017).

Short-lived species such as small pelagic fish transition between life stages more rapidly than longer-lived species. Their life cycle is characterized by strong seasonal variability in demographic processes such as growth, natural mortality and maturity (and recruitment consequently) (Cole and McGlade, 1998). Small pelagic fish like sardines play an important role in marine food webs as being a key linkage from low trophic levels to high trophic levels (Cury et al., 2000). Over the past two decades, sardines in the Bay of Biscay (*Sardina pilchardus*) have shown a decrease in size-at-age, weight-at-age, age 1 survival, body condition and growth at age (Boëns et al., 2021; Bordes et al., Under review; Doray et al., 2018; Véron et al., 2020). The main hypothesis is a bottom-up control of phenotypic response due to a change in the quality and quantity of trophic availability occurring at different life stages (Grandrémy, 2023; Menu et al., 2023), including potential changes in mortality and growth at different life stages.

However, the underlying demographic mechanisms driving those changes in population dynamics remain unclear. Additionally, like the majority of stock assessment in fisheries sciences (Vert-pre et al., 2013), the current assessment model for sardine in the Bay of Biscay (conducted using Stock synthesis (ICES and WGHANSA, 2024; Methot and Wetzel, 2013)) considers natural mortality is stationary and models growth implicitly via pre-specifying weight-at-age on empirical data (ICES and WGHANSA, 2024). Such practices that may lead to bias in model estimates (Correa et al., 2023). Those limits preclude the understanding of mechanisms driving changes in population dynamics and the provision of reliable scientific advice for fisheries management.

Recently, as a first step towards shedding light on these mechanisms underlying changes in sardine growth and mortality, Bordes et al. (Under review) developed a state-space life cycle model for the sardine population in the Bay of Biscay. In this recent study, the authors inferred for the first time the temporal variability in natural mortality and growth at each life stage. Additionally, this life

cycle model was used to disentangle the influence of density dependence, size-dependence and environmental factors on the population dynamics of small pelagic fish. However, this model suffered from several weaknesses. First, estimation of growth was quite stable over the time series for all ages, whereas it is expected that growth might strongly vary for early ages (Véron et al., 2020). Secondly, no evidence of the tested environmental indices on natural mortality or growth was found. We suspect that these limitations are due to the incorrect time scale (annual resolution) used by Bordes et al. Indeed, sardines are a short-lived species undergoing rapid demographic transitions – such as growth, mortality– that can occur within a single year.

To be properly understood, sardine population dynamic needs thus to be studied on a seasonal scale. Indeed, in the Bay of Biscay, sardines exhibit marked seasonal variation in body condition, along with an age-specific decreasing trend in condition over time (Véron et al., 2020). Maximum body condition is typically reached at the end of summer, following the productive and spawning season. This reflects a broader pattern observed in small pelagic species, which experience alternating productive and unproductive periods tied to pronounced seasonal fluctuations in food availability. In particular, winter is characterized by reduced light and colder temperatures, which limit plankton productivity and make food (phytoplankton and zooplankton) scarce. This seasonality has critical implications for sardine bioenergetics. In the Bay of Biscay, four distinct productivity seasons are recognized: a low-productivity winter, a nutrient-limited bloom in spring, stratified low-productivity summer conditions, and a secondary bloom in autumn (Longhurst, 2010). Sardines typically spawn from autumn to spring, with limited activity during mid-winter (Coombs et al., 2006; Stratoudakis et al., 2007), making the accumulation of energy reserves from spring to autumn critical for sustaining metabolic demands during spawning and overwintering periods (Gatti et al., 2018; Rosa et al., 2010).

This work aims at better understanding the seasonal changes in sardine population dynamics, with a focus on variations in abundance and size structure. We have developed two models, a seasonal population dynamics model and a seasonal growth model, where each year is composed of two seasons due to the seasonal environments: a productive season (April to September) characterized by higher temperature and high plankton productivity, increasing food availability for sardines, and unproductive season (October to March) characterized by reduced light and colder temperatures, which limit plankton productivity and make food scarce. The seasonal population dynamic model tracks abundances for each year and season and allows to infer seasonal changes in mortality. The growth model tracks weight at age for each year and season and allow to infer seasonal changes in growth for each age. These integrated population models integrate heterogenous data for each season combining spring and fall surveys and seasonal fisheries data. Using these seasonal models, we will address 4 questions:

[Q1] Does using data from a different season change our perception of the state of the stock?

Population dynamics models for sardines relies mainly on PELGAS survey (spring) (ICES, 2024; Menu et al., 2023; Bordes et al., Under review), and so the key parameters for management are estimated from PELGAS survey data (spring). For the first time we compiled data from another survey, JUVENA, occurring in fall. As an exploratory step in understanding seasonality in sardine population dynamic, we investigate in [Q1] if a population dynamics model based only on fall data will change the estimates in key parameters, such as recruitment, fishing mortality, natural mortality and SSB. We provide for

the first time a comparison in key management quantities between a yearly population dynamic model fitted to PELGAS survey (spring) and to JUVENA survey (fall).

[Q2] Can we estimate seasonal varying growth and mortality for sardines in the Bay of Biscay?

Sardines in the Bay of Biscay have decreased in length and weight at all ages (Doray et al., 2018; Véron et al., 2020) and experience higher mortality since 2012, especially on age 1 (Boëns et al., 2021; Bordes et al., Under review), as well as a decline in condition (Véron et al., 2020). Thus, we expect to estimate time varying natural mortality and growth with strong patterns (increasing for mortality and decreasing for growth) and variability for early ages (1 and 2 in particular), and this for each season. To do so we developed for the first time a seasonal model integrating data from both the JUVENA and PELGAS surveys.

[Q3] Are growth higher during productive seasons and mortality higher during unproductive seasons?

Using the estimates from the seasonal model, we expect higher survival and growth during productive seasons, and increased mortality with reduced growth during unproductive ones.

Also, temperate species adopt overwintering strategies that involve reduced activity and minimal feeding, relying instead on stored energy reserves (Schultz and Conover, 1999, 1997; Van Deurs et al., 2010). We then expect lower growth during unproductive season.

Additionally maintenance metabolism in fish scales with both temperature and body size (Van Deurs et al., 2011). Consequently, smaller individuals face higher mass-specific metabolic demands and are more vulnerable to starvation during winter when feeding opportunities are limited (Van Deurs et al., 2011). We then expect to estimate higher mortality during unproductive season, and more variability for young fish (especially age 1).

[Q4] Is higher mortality during unproductive seasons preceded by lower growth during the productive seasons?

The ability to survive unproductive periods depends on reaching a critical threshold size before winter, above which individuals possess sufficient reserves to buffer against starvation (Van De Wolfshaar et al., 2008; Van Deurs et al., 2011). We expect sardines to follow such a strategy and therefore mortality to be higher during unproductive seasons when growth has been poor during previous productive seasons.

2. Material and methods

The modelling approach consists of statistical models (growth and population models) with limited data driven by key demographic processes. Some processes cannot be observed and are inferred such as fishing mortality, natural mortality, growth and recruitment. Other are predefined based on data or expertise such as maturity and survey selectivity.

In this section we will first describe the multiple sources of data, their yearly and seasonal resolution, and the predefined demographic parameters. Then we will present the different models (yearly

defined, seasonally). And we will present how we modelled the time varying key demographic parameters using random effects.

Growth model (G-SEAS) is seasonal. Population dynamics models are annual (MY-PEL for the annual model informed by the PELGAS survey, MY-JUV for the annual model informed by the JUVENA survey), to be able to compare with the current models used for management, and seasonal (M-SEAS). Figure 1 illustrates the conceptual structure of the three population dynamic models. Models MY-PEL, MY-JUV and M-SEAS track abundance $N_{t,a}$ and allow to estimate natural mortality $M_{t,a}$ and fishing mortality $F_{t,a}$ where *t* corresponds to year for MY-PEL and MY-JUV and to season for M-SEAS and *a* corresponds to age for all three models. Although MY-PEL and MY-JUV share the same yearly framework (Fig. 1a), the timing of catches relative to the survey differs. For sardine in the Bay of Biscay, most of the annual catches occur during summer. In MY-PEL, the PELGAS survey occurs in May, before the majority of the annual catches. Thus, the catches for year *t* correspond to fishing mortality that occurs between year *t* and year *t+1*. However, for MY-JUV, the JUVENA survey occurs in September/October, after most of the annual catches. To capture fishing mortality between year *t* and *t+1*, the relevant catches are therefore those of year *t+1*. The seasonal model M-SEAS (Fig. 1b) expands the structure to a seasonal framework, where two surveys per year (PELGAS in spring and JUVENA in autumn) inform the dynamics within the same annual cycle. Finally model G-SEAS uses the same seasonal framework as M-SEAS to track weight-at-age $W_{t,a}$ and estimate growth $G_{t,a}$.

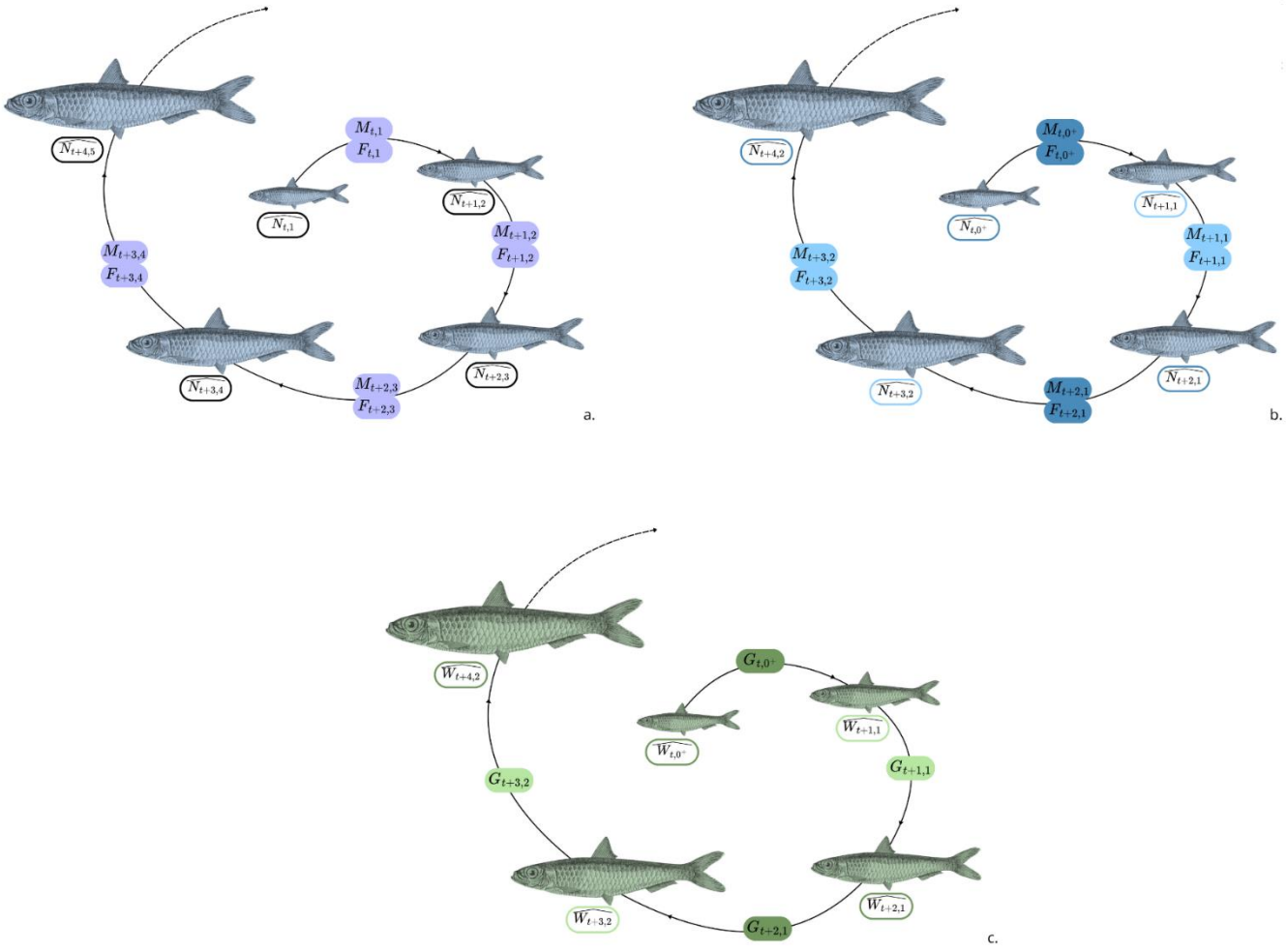

Fig. 1: Simplified schematic representation of the population dynamics models. a. Yearly models using PELGAS (MY-PEL) or JUVENA (MY-JUV) data. b. Seasonal model tracking abundance (M-SEAS). c. Seasonal model tracking weight (G-SEAS). For the seasonal models, the lighter color represents the productive season while the darker color represents the unproductive season.

2.1 Data and predefined demographic parameters

The data presented in this section correspond to the observations that will inform the model through different likelihood functions, whereas the predefined parameters represent inputs treated as known variables in the models.

The size-structured data provided by the JUVENA campaign are only available from 2010 onwards, constraining the seasonal models to the same temporal range.

2.1.1 Data

The Bay of Biscay (43-48◦N, 8–0.1◦W) is an oceanic bay extending from Brittany, in the north-west of France, to the Cape Finisterre, in the north-west of Spain. Its hydrography is influenced by the open ocean as well as by large rivers such as the Loire (47°N,2°W) and the Gironde (45.5°N,1°W) (Koutsikopoulos and Le Cann, 1996).

The sardine population in the Bay of Biscay inhabits the continental shelf (Fig.6), where it completes its entire life cycle and is exploited by the fishery.

2.1.1.a Fisheries Data

Sardine is targeted by a French fishery in the northern part of the Bay of Biscay and a Spanish one in the southern part. Hence, the fisheries data used in this study include contributions from both countries but are restricted to the study area, specifically the French section of the Bay of Biscay continental shelf. These data provide information on age composition (as proportions) (Fig. 2c and 2d), and total catch (in tons) (Fig. 2a and 2b).

The data is available on a quarterly basis (e.g, the first quarter spans January to March). For annual models we aggregated data yearly. When applying a seasonal temporal resolution, two seasons were defined: Season 1 (the productive season), spans April to September, and Season 2 (the unproductive season) spans October to March. Consequently, Season 1 corresponds to the aggregation of the quarters 2 and 3, while Season 2 corresponds to the aggregation of quarter 4 and quarter 1 of the following year. Age compositions were reconstructed by weighing the number of fish at age by the corresponding seasonal catch.

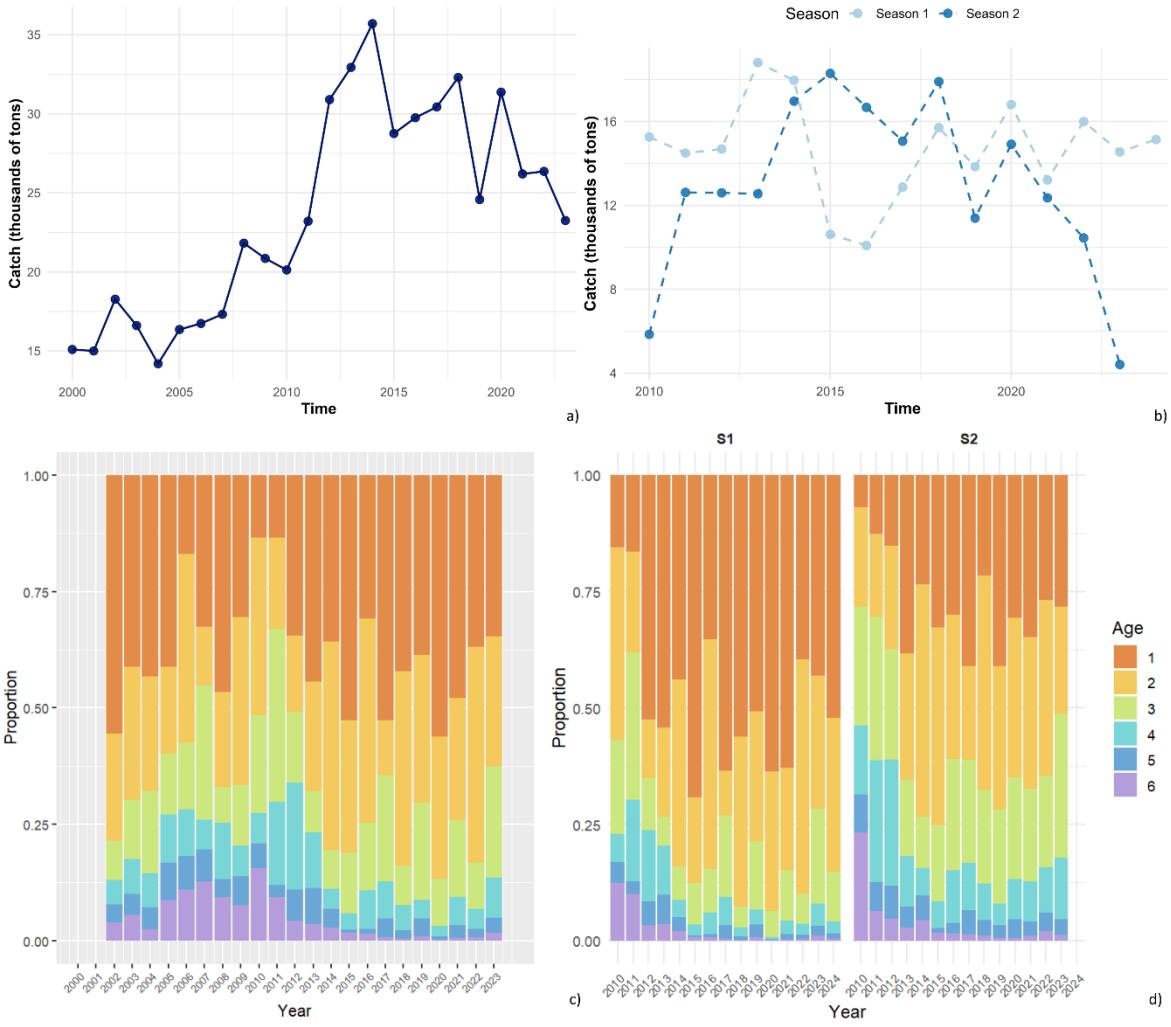

Fig. 2: Fisheries data informing the models. a. Annual catch data. b. Seasonal catch data. c. Annual age composition data. d. Seasonal age composition data (S1: season 1 and S2: season 2)

2.1.1.b Survey Data

Data used in this study were obtained from two integrated scientific surveys of the Bay of Biscay pelagic ecosystem: the PELGAS survey in spring (May) and the JUVENA survey in autumn (end of September). Both surveys aim, among other objectives, to assess the abundance, biomass, and the size structure of small pelagic fish communities in the Bay of Biscay using an acoustic-trawl methodology (Doray et al., 2021). The PELGAS survey, unlike JUVENA, also provides information on the age structures of the small pelagic fish populations.

Since 2000, PELGAS has been conducted over the French continental shelf of the Bay of Biscay (see Fig. 3) by Ifremer, in collaboration with La Rochelle University and CNRS (Doray et al., 2018).

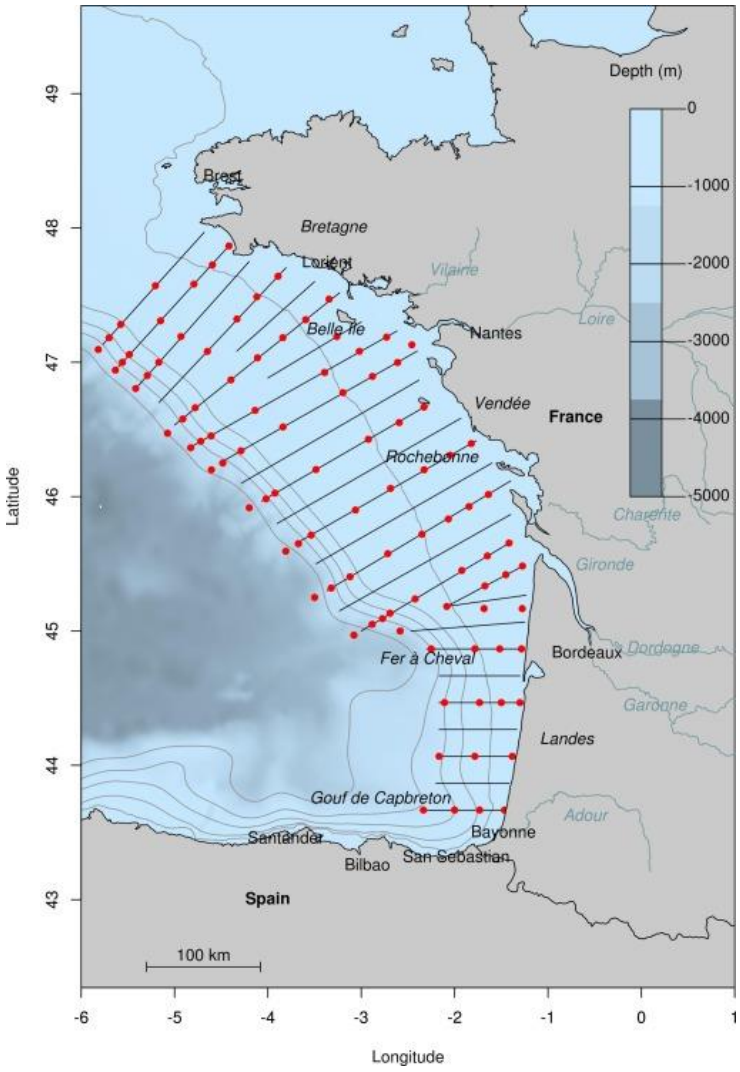

Fig. 3: PELGAS survey sampling scheme (solid lines: systematic line transects, red dots: hydrobiology stations, light grey lines: 100, 200, 300, 400, 500m isobaths.) (Doray et al., 2018)

The JUVENA survey, initiated in 2003 and coordinated between AZTI and IEO, focuses on juvenile small pelagic fish and covers both the Spanish and French coasts (Boyra et al., 2003). For this study, only data collected within the French continental shelf of the Bay of Biscay were used.

Both surveys employ acoustic techniques, using echo sounders mounted on the vessel hull to emit short ultrasonic pulses into the water column. When fish are present, part of the signal is backscattered and recorded by the echo sounder. Because pelagic fish often reside in surface layers (0-10m) at night – beyond the range of the sounder – acoustic surveys are conducted during daylight hours.

Biomass estimates are obtained through echo-integration, which quantifies the total acoustic energy backscattered by fish within a defined area (Simmonds et al., 2005).This is done at the scale of the Elementary Distance Sampling Unit (ESDU), equivalent to one nautical mile of linear acoustic sampling (Doray et al., 2018). Since the acoustic signal reflects mixed-species assemblages, pelagic trawls (4-6 per day) are regularly performed to identify species and size and age composition. These data are then used to allocate species and size or age structures to the corresponding acoustic signals at the EDSU level (Doray et al., 2021).

Each of these surveys can be used to inform a population dynamics model with annual resolution. However, within the seasonal framework adopted in this study, each survey is also used to delimit the two seasons defined earlier. PELGAS, conducted in spring, marks the end of the unproductive season and the beginning of the productive season, while JUVENA, conducted in autumn, marks the end of the productive season and the beginning of the unproductive season.

Both surveys provide a total abundance index. PELGAS reports abundance in terms of biomass (Fig. 4b), accounting for ages 1 to 6+ while JUVENA provides abundance in numbers (Fig. 4a). Because JUVENA focuses primarily on juvenile fish, in addition of estimates of abundance for adult life stages (age 1 to 6+), it also provides estimates of age-0 abundance, which can be used as a recruitment index in the model – an approach already applied in the anchovy stock assessment (Boyra et al., 2003).

Additionally, PELGAS includes age composition data (Fig. 4c) which are essential for informing age-structured models. In contrast, JUVENA provides only size composition data (Fig. 4d), over a time series spanning from 2010 to 2024. This creates the need to construct an age-length key to derive age composition from JUVENA data, ensuring consistency across both surveys when informing the model.

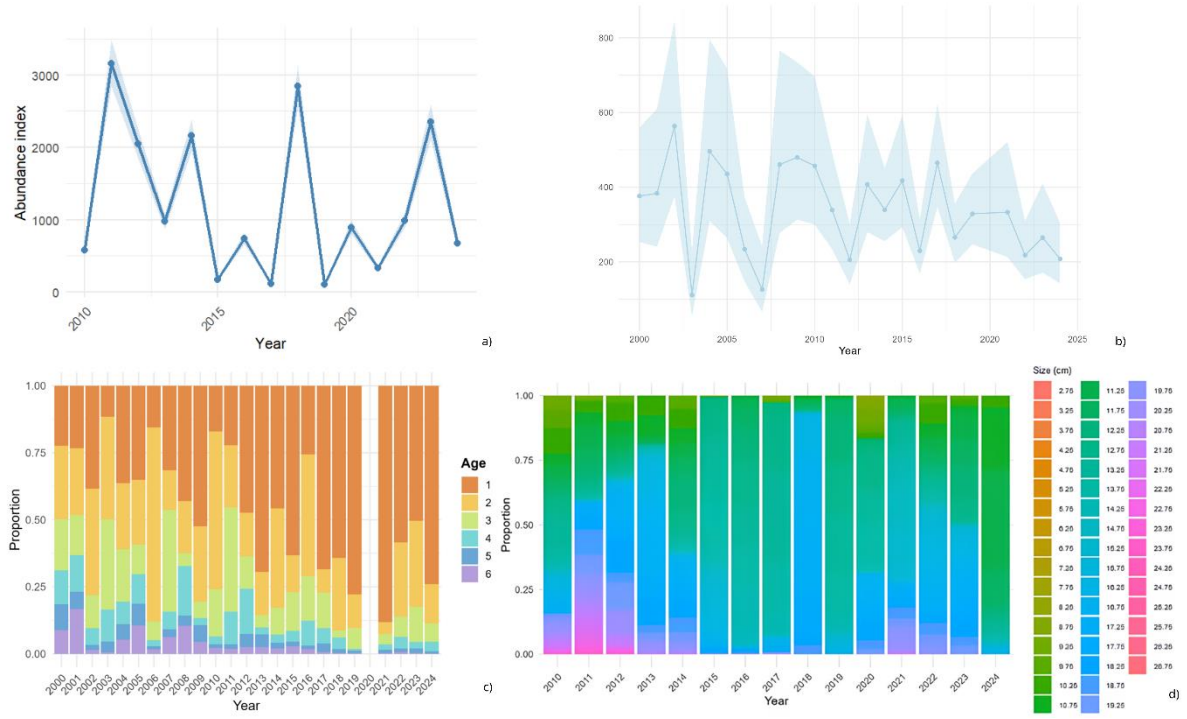

Fig. 4. Abundance index and age/size composition. a. Abundance index (for ages 1-6+) in number of fish from the JUVENA survey. b. Abundance index (for ages 1-6+) in biomass from the PELGAS survey. c. Age composition data from the PELGAS survey informing a yearly model or the odd-numbered seasons of a seasonal model (the survey could not be conducted in 2020 because of COVID). d. Size composition data from the JUVENA survey before transformation in age composition

2.1.1.c Pre-processing

As previously mentioned, constructing an age-length key was necessary to derive age composition from JUVENA data. Since the JUVENA survey is conducted in autumn, we initially chose to use data from the EVHOE survey – also conducted in the Bay of Biscay in autumn (though later in the year, in

November), by Ifremer – to build the key for sardine. However, we noted that the length values were substantially lower than expected for that time of year, which might be explained by the difference in fishing gears and sampling scheme used in the two campaigns, EVHOE being a bottom trawl survey which does not aim to study pelagic fish. Thus, we decided to also incorporate data from fisheries (further details are provided in the Supplementary Material 1). Data from the years 2010 to 2024 were selected and used to establish the age-length relationship shown below (Fig. 5).

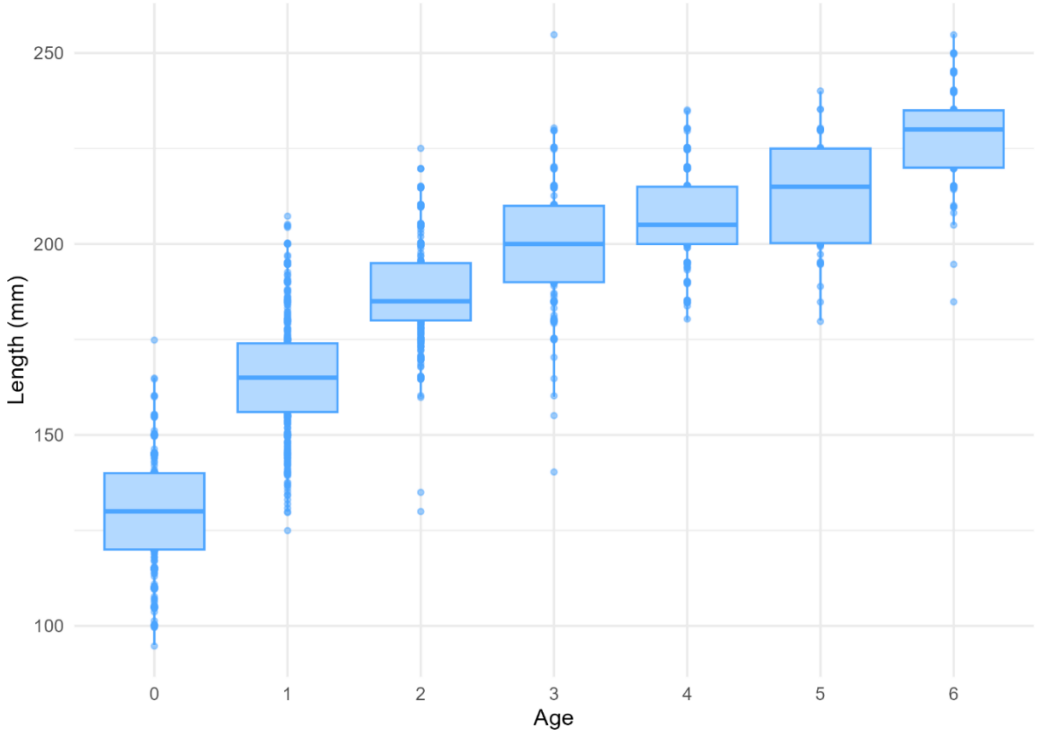

Fig. 5: Length at age data from the aggregation of EVHOE and fishery data

One age-length key, common for all years, was generated using the FSA package in R (Ogle et al., 2015) from the previously presented dataset. Initially, a contingency table is constructed to represent the number of observations for each combination of age and length class. Subsequently, this table is converted into a matrix of proportions, where, for each length class, the values represent the relative frequency of individuals at each age. This transformation provides the conditional probability of belonging to a given age given the length class.

The JUVENA size classes were first transformed to align with those used in the age-length key before applying it to the annual numbers-at-size data from JUVENA. By multiplying the age-length key with each year's size distribution, we obtained estimated numbers-at-age. Given that the JUVENA survey targets juvenile fish, the abundance of age-0 individuals was extracted separately and used as an annual recruitment index. The abundances for ages 1 to 6+ were converted into age composition by dividing each number-at-age by the total abundance across these age classes.

2.1.2 Predefined demographic parameters

For all models, certain parameters were predefined based on available data or expert knowledge. Maturity, defined as the proportion of mature individuals by age, was defined using survey data: for

the productive season, PELGAS data were used, while for the unproductive season, the same sources of data used for the age-length key (EVHOE and fishery data) were applied to define maturity, due to the absence of maturity data from the JUVENA survey. To derive weight-at-age data from surveys (Fig. 6a), again, PELGAS data were used for the productive season and a mean of EVHOE and fishery data for the unproductive season.

In addition, weight-at-age from fisheries data was available on a quarterly basis and was aggregated accordingly to the temporal resolution used in the model, using catch-weighted means (Fig. 6b).

Survey selectivities were defined based on scientific expertise. For the JUVENA survey, which targets individuals from age 0, selectivity was assumed to be 1 across all age classes. For the PELGAS survey, selectivity was set to 0 for age 0 (as PELGAS does not sample juveniles), 0.9 for age 1 (reflecting that approximately 10% of age-1 sardines are thought to remain nearshore and outside the survey area (Doray et al, personal com), and 1 for ages 2 and older.

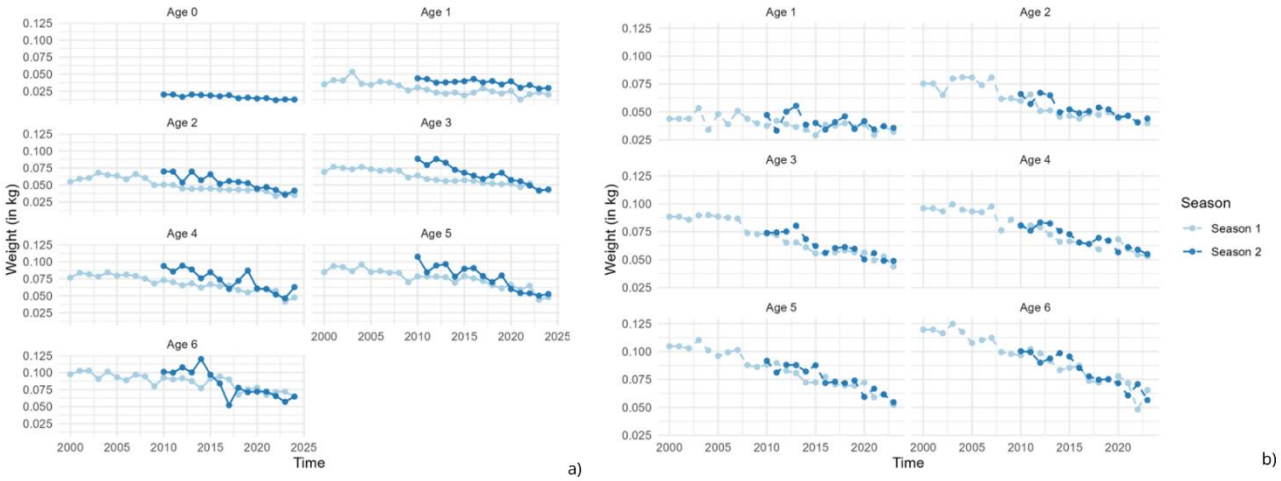

Fig. 6: Weight-at-age data. a. From the PELGAS survey (season 1) and the aggregation of EVHOE and fishery data (season 2). b. From the fisheries.

In the population dynamics models (abundance-tracking models), weight-at-age data were treated as predefined parameters. In contrast, the growth population model (growth-tracking model) incorporated weight-at-age data from the survey as observed data within the likelihood function, allowing the model to estimate growth parameters (see section 2.2.1.b).

2.2. State space population dynamics models to infer time varying demographic parameters

2.2.1 General model outlines

The modelling framework developed in this study, which considers the Bay of Biscay sardine population as a single stock and assesses the effects of temporal resolution on population dynamics inference included different steps.

1. Step 1: As a first step, we developed a yearly defined population dynamics model (MY-PEL). This master thesis was conducted at the same time as the WGHANSA annual meeting (ICES and WGHANSA, 2025), providing an opportunity to present a yearly state space model as a

potential benchmark model for the sardine stock in the Bay of Biscay. The model was shared with WGHANSA, along with a comparison of its outputs with those from the current assessment model (see Supplementary Materials 6 for details).

Our model relies on the same data (from PELGAS survey) as the current assessment but does not include egg abundance (see Discussion). It shows several improvements over the existing model (SS3). First, the state-space framework within TMB allows greater flexibility than SS3. Second, fishing mortality (F) is estimated as time-varying for each age class, implicitly capturing changes in selectivity over time (Nielsen and Berg, 2014). Finally, the model allows the estimation of time-varying natural mortality.

2. Step 2: We used the same yearly population dynamics model as described previously (Step 1), but incorporating JUVENA survey data (model MY-JUV). The use of this survey in such a model is novel and represents a significant improvement, as it provides a direct recruitment index. Indeed, JUVENA primarily targets juvenile individuals and thus offers an abundance index for age-0 fish — something that the PELGAS survey does not provide. However, unlike PELGAS data, which is age-structured, JUVENA data is size-structured. As a result, a transformation using a length–age key was necessary to integrate JUVENA data into the model. The model allows then to estimate recruitment at age 0 for the first time and time varying natural mortality. Key outputs (recruitment, time varying mortality, recruitment, spawning stock biomass) were compared between MY-PEL and MY-JUV.

3. Step 3: To address our three research questions (Q2-Q3-Q4), we developed two seasonally state space models. The first model is a seasonal population dynamics model (M-SEAS) that combines data and processes from both MY-PEL and MY-JUV. The model allows to infer recruitment at age 0, and seasonal varying mortalities (both fishing and natural mortalities). The second model is a growth model (G-SEAS) that estimates seasonal and yearly varying growth. These models integrate data from both the PELGAS and JUVENA surveys, with each survey informing a different season of the year.

Because the JUVENA size structure data were only available from 2010, the models using data from JUVENA have shorter time series than the PELGAS yearly model. The time series covered by each model is displayed in Table 1.

Table 1: Time series covered by each model

Model	Nature of the model	Data source	Data type	Temporal resolution	Time series
MY-PEL	Pop dyn	PELGAS	Abundance index Age compositions Maturity Weight at age	Yearly	2000-2024

MY-JUV	Pop dyn	JUVENA	Abundance index Age compositions Maturity Weight at age	Yearly	2010-2023
M-SEAS	Pop Dyn	PELGAS and JUVENA	Abundance index Age compositions Maturity Weight at age	Seasonal	2010-2024
G-SEAS	Growth model	PELGAS and JUVENA	Weight at age	Seasonal	2010-2024

2.2.2 MY-PEL: A yearly defined population dynamics model based on PELGAS data to infer recruitment and mortalities (step 1)

The model tracks sardine abundance across all ages (from 1 to 6) using an annual time step (from 2000 to 2024). Transitions in abundance between consecutive ages are governed by survival rates resulting from the combined effects of age-specific fishing and natural mortality.

Compared to the current SS3 assessment model, the main originality of this model lies in the flexibility provided by the state-space framework, the inclusion of time-varying natural mortality, and the estimation of fishing mortality by age. Another key distinction is the exclusion of egg abundance data, which are not incorporated here (see Discussion for details).

The model relies on a classical population dynamics structure. Log-abundance for a given year and a given age is defined as the log abundance of the previous age and previous year, minus the corresponding natural and fishing mortality. Catches are estimated using the Baranov catch equation. Recruitment and natural morality are treated as random effects, modelled using a log-linear formulation, while fishing mortality is estimated as a random walk process.

As described in previous sections, the model is informed by annual data from the PELGAS survey and fisheries through lognormal and Dirichlet likelihoods. Specifically, the data include annual abundance indices, total annual catches, and age compositions for both the survey and the fishery (Table 1).

More details about the model structure are available in Supplementary Material 2.

2.2.3 MY-JUV: A yearly defined population dynamics model based on JUVENA data to infer recruitment and mortalities (step 2)

As with the previous model, this version tracks sardine abundance across all age classes using an annual time step. It relies on the same classical population dynamics structure and incorporates the same random effects.

However, as previously mentioned, this model is informed by the JUVENA survey, which introduces a key difference: the integration of age-0 individuals into the population dynamics. This provides direct information on recruitment and enhances early life stage representation, which was absent in the model informed by PELGAS.

A notable limitation is that JUVENA data are only available from 2010 to 2024, which shortens the time series and constrains the temporal window over which population dynamics can be analysed with this model.

2.2.4 Stage based seasonal models (step 3)

The temporal resolution selected for these models is seasonal, with each season defined as a six-month period. Based on existing literature on sardine (*Sardina pilchardus*) in the Bay of Biscay, and considering the constraints imposed by the number of available scientific surveys, the year was divided into two distinct seasons:

- Season 1 (S1; April to September): beginning informed by data from the PELGAS survey, which typically occurs in Spring and targets adult pelagic species;
- Season 2 (S2; October to March): beginning informed by the JUVENA survey, conducted in Autumn and primarily focused on juvenile fish.

Due to the aforementioned limited availability of JUVENA data (2010–2024), both seasonal models were restricted to this time series.

2.2.4.a M-SEAS – A seasonal population dynamics model to infer recruitment, and seasonal mortalities

The model tracks the dynamics of abundance across the life cycle where each life stage is defined as a unique combination of age and season. Changes in abundance between consecutive life stages are driven by a survival rate resulting from a combination of age-dependent fishing and natural mortality. The difference with the first model presented resides in the seasonal temporal resolution, as well as the inclusion of age 0 in the population dynamics.

The model can be represented as follows (Fig. 7):

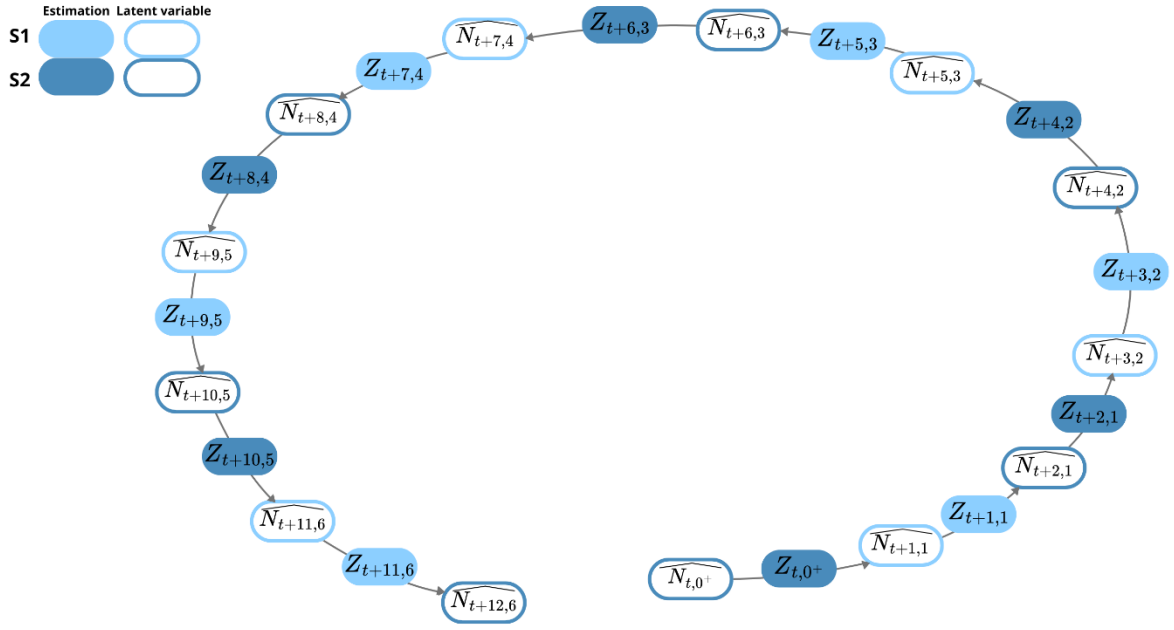

Fig. 7: State-space model tracking abundance (N). Z denotes total mortality, defined as the sum of natural mortality (M) and fishing mortality (F)

Let $N_{t,a}$ denote the estimated abundance at age *a* (ranging from 0 to 6+) and time step *t* (ranging from 1 to 30, i.e the product of 2 seasons by 15 years), where odd-numbered time steps correspond to S1 and even-numbered time steps correspond to S2.

For ages 1 to 6+, log abundance was calculated recursively as the log abundance for previous life stage minus corresponding natural ($M_{t,a}$) and fishing ($F_{t,a}$) mortality. When *t* is odd, the next season is still within the same year, so the fish remain the same age. When *t* is even, the year changes, and the fish age by one year:

$$\log \widehat{N_{t+1,a}} = \begin{cases} \log \widehat{N_{t,a}} - M_{t,a} - F_{t,a} & if\ t\ is\ odd \\ \log \widehat{N_{t,a-1}} - \log M_{t,a-1} - F_{t,a-1} & if\ t\ is\ even \end{cases} \quad (1)$$

At the initial time step t=1, the model is initialized for ages 1 to 6+:

$$\log \widehat{N_{1,a}} = \mu_{N_{0,a}} \qquad age\ a = 1, \dots, 6 \quad (2)$$

Recruitment is assumed to occur at age 0+ during season 2. Thus, for even-numbered time steps, the abundance of recruits was modelled with a year-specific (y = 1, … ,15) random effect:

$$\log \widehat{N_{t,0}} = \mu_R + \varepsilon_{R_y} \qquad if\ t\ is\ even \quad (3)$$

The natural mortality rate was modelled using a log-linear formulation:

$$\log M_{t,a} = \log \mu_{M_a} + \varepsilon_{M\,t,a} \quad (4)$$

Again, estimated index of abundance, in number if fish $\widehat{I_{t,a}}$ and in biomass $\widehat{I_{w_{t,a}}}$, and spawning biomass at age $\widehat{SB_{t,a}}$ were calculated from the estimated log abundance for ages 1 to 6+:

$$\widehat{I_{t,a}} = \begin{cases} \widehat{N_{t,a}} * s_a * q_{PEL} & if\ t\ is\ odd \\ \widehat{N_{t,a}} * s_a * q_{JUV} & if\ t\ is\ even \end{cases} \qquad (in\ number\ of\ fish) \quad (5)$$

$$\widehat{I_{w_{t,a}}} = \begin{cases} \widehat{N_{t,a}} * s_a * q_{PEL} * W_{t,a} & if\ t\ is\ odd \\ \widehat{N_{t,a}} * s_a * q_{JUV} * W_{t,a} & if\ t\ is\ even \end{cases} \qquad (in\ biomass) \quad (6)$$

$$\widehat{SB_{t,a}} = \widehat{N_{t,a}} * mat_{t,a} * W_{t,a} \qquad (7)$$

Where s_a corresponds to PELGAS selectivity for age *a* for odd-numbered seasons and JUVENA selectivity for age *a* for even-numbered seasons, q_{PEL} and q_{JUV} correspond to the catchability of the PELGAS and JUVENA surveys respectively, and $W_{t,a}$ denotes mean weight at age *a* for season *t*.

An annual recruitment index ($\widehat{I_{rec_t}}$ in number of fish, $\widehat{I_{w_{rec_t}}}$ in biomass) was calculated from even-numbered seasons age 0 estimated abundance:

$$\widehat{I_{rec_t}} = \widehat{N_{t,0}} * s_0 * q_{JUV} \qquad (in\ number\ of\ fish) \quad (8)$$

$$\widehat{I_{w_{rec_t}}} = \widehat{N_{t,0}} * s_0 * q_{JUV} * W_{t,0} \qquad (in\ biomass) \quad (9)$$

Total index of abundance and spawning biomass were then obtained by summing the age-specific values over ages 1 to 6:

$$\widehat{I_t} = \sum_{a=1}^{6} \widehat{I_{t,a}} \qquad (in\ number\ of\ fish) \qquad (10)$$

$$\widehat{I_{w_t}} = \sum_{a=1}^{6} \widehat{I_{w_{t,a}}} \qquad (in\ biomass) \qquad (11)$$

$$\widehat{SB_t} = \sum_{a=1}^{6} \widehat{SB_{t,a}} \qquad (12)$$

The estimated catches in number of fish were calculated using a Baranov equation:

$$\widehat{C_{t,a}} = \frac{F_{t,a}}{F_{t,a}+M_{t,a}} * N_{t,a} * (1 - e^{-M_{t,a}-F_{t,a}}) \qquad (13)$$

And converted into biomass using weight-at-age data from the fisheries:

$$\widehat{C_{w_{t,a}}} = C_{t,a} * W_{f_{t,a}} \qquad (14)$$

Fishing selectivity at age *a* for time step *t* was calculated as the fishing mortality at age *a* for time step *t* divided by the total fishing mortality in that time step:

$$s_{fishery_{t,a}} = \frac{F_{t,a}}{F_t} \qquad (15)$$

In this model, the following were estimated as fixed effect parameters:

- q_{PEL} : catchability of the PELGAS survey,
- q_{JUV} : catchability of the JUVENA survey,
- μ_R : mean log abundance at age 0.
- $\mu_{N_{0,a}}$: initial log abundance for each age.

And the following were fixed to a given value based on expertise:

- $\log \mu_{M_a}$: log of the age-specific mean natural mortality rate (fixed according to the natural mortality values used by the assessment model),
- $\sigma_{\log C_{obs}}$: observation error for catches,
- θ_1: Dirichlet parameter for the survey age composition for season 1,
- θ_2: Dirichlet parameter for the survey age composition for season 2,
- θ_F: Dirichlet parameter for the catches age composition.

The model includes random effects on recruitment abundance, natural and fishing mortality using a lognormal distribution for recruitment abundance and natural mortality:

$$\varepsilon_{M_{t,a}} \sim N\left(0, \sigma_{\log \varepsilon_M}\right) \quad (16)$$

$$\varepsilon_{R_t} \sim N(0, \sigma_{\log \varepsilon_W}) \quad (17)$$

And a random walk for fishing mortality:

$$\log F_{t,a} \sim \begin{cases} N(0,1), & t = 1 \\ N\left(\log F_{t-1,a}, \sigma_{\log \varepsilon_{F_a}}\right), & t > 1 \end{cases} \quad (18)$$

These capture inter-annual variation not explained by fixed effects. The use of a random walk for each age allows to implicitly estimate time varying selectivity (Nielsen and Berg, 2014).

The model is informed by seasonal index of abundance and age composition (i.e., proportion of each age for a given season, calculated by dividing number at age by total number of fish) obtained from scientific surveys, and seasonal catch and age composition for the fisheries.

The observations were incorporated using a lognormal likelihood or a Dirichlet:

Table 2: Likelihoods for the M-SEAS model

Notation	Data type	Unit	Likelihood
C_t	Seasonal fisheries catch	Tons	$\log C_t \sim N(\log \hat{C}_t, {\sigma_{\log C}}^2)$
I_t	Seasonal index of abundance	Number of fish for even seasons and biomass for odd seasons	$\log I_t \sim \begin{cases} N(\log \hat{I}_{w_t}, {\sigma_{\log I}}^2), & if\ t\ is\ odd \\ N(\log \hat{I}_t, {\sigma_{\log I}}^2), & if\ t\ is\ even \end{cases}$

Notation	Data type	Unit	Likelihood
I_{rec_t}	Annual index of recruitment	Number of fish	$\log I_{rec_t} \sim N(\log \widehat{I_{rec_t}}, 0.1^2)$
$p_{AC_{t,a}}$	Age composition for the survey	Proportion	$p_{AC_{t,a}} \sim \begin{cases} \text{Dirichlet}(\theta_1 \cdot \widehat{p_{AC_{t,a}}}), & if\ t\ is\ odd \\ \text{Dirichlet}(\theta_2 \cdot \widehat{p_{AC_{t,a}}}), & if\ t\ is\ even \end{cases}$
$p_{AC\_F_{t,a}}$	Age composition for the fisheries	Proportion	$p_{AC\_F_{t,a}} \sim \text{Dirichlet}(\theta_F \cdot \widehat{p_{AC\_F_{t,a}}})$

2.2.4.b G-SEAS: A seasonal model to estimate seasonal growth

The model tracks the dynamics of weight across the life cycle where each life stage is defined as a unique combination of age and season. Changes in weight between consecutive life stages are driven by a pseudo-growth rate that reflects the net change in mean population weight resulting from a combination of average somatic growth and weight-selective mortality.

The model can be represented as follows:

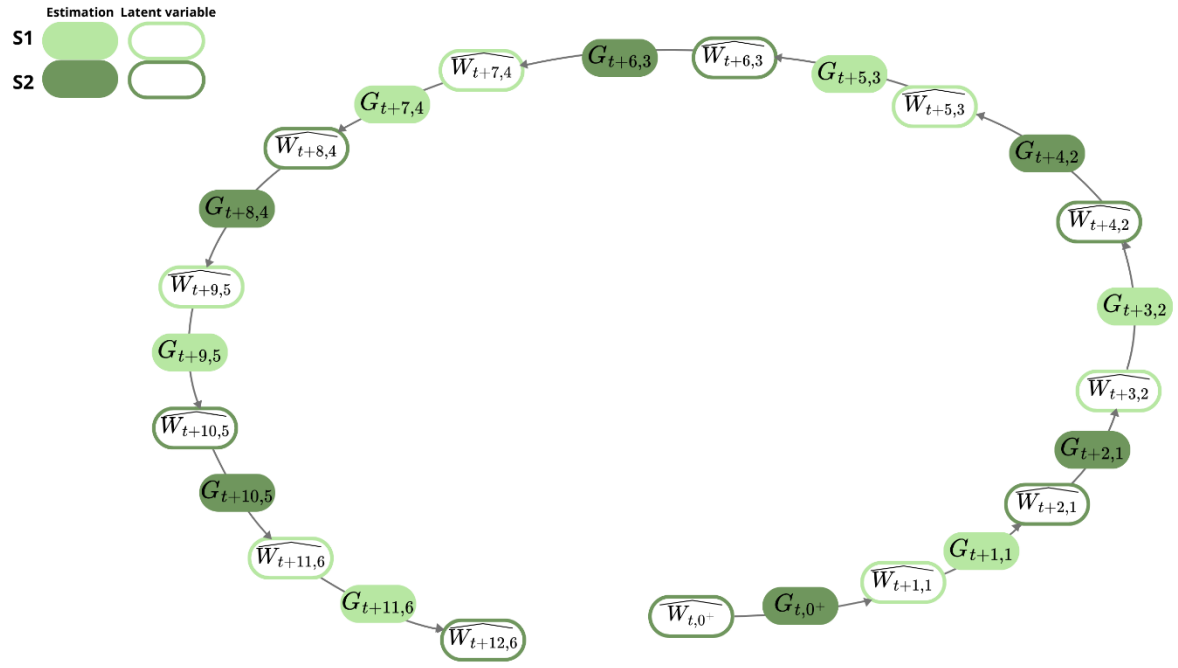

Fig. 8: Life-cycle state-space model tracking weight

Let $W_{t,a}$ denote the estimated mean weight-at-age *a* (ranging from 0 to 6+) and time step *t* (ranging from 1 to 30), where odd-numbered time steps correspond to S1 and even-numbered time steps correspond to S2.

For ages 1 to 6+, log of mean weight was calculated recursively as the sum of the log of weight at the previous life stage and the log of corresponding pseudo-growth rate $G_{t,a}$:

$$\log \widehat{W_{t+1,a}} = \begin{cases} \log \widehat{W_{t,a}} + \log G_{t,a} & if\ t\ is\ odd \\ \log \widehat{W_{t,a-1}} + \log G_{t,a-1} & if\ t\ is\ even \end{cases} \quad (19)$$

At the initial time step t=1, the model was initialized using the observed mean weight-at-age data:

$$\log \widehat{W_{1,a}} = \mu_{W_{0,a}} \qquad age\ a = 1, \dots, 6 \quad (20)$$

Recruitment is assumed to occur at age 0+ during season 2. Consequently, for even-numbered time steps, the mean weight of recruits was modelled with a year-specific (y = 1, … ,15) random effect:

$$\log \widehat{W_{t,0}} = \mu_W + \varepsilon_{W_y} \qquad if\ t\ is\ even \quad (21)$$

The pseudo growth rate was modelled using a log-linear formulation:

$$\log G_{t,a} = \log \mu_{G_{s,a}} + \varepsilon_{G\,t,a} \quad (22)$$

Here, $\mu_{G_{s,a}}$ represents the age and season-specific mean pseudo-growth rate, and $\varepsilon_{G\,t,a}$ is a random effect accounting for stochastic temporal variation.

In this model, the following were estimated as fixed effect parameters:

- $\log \mu_{G_{s,a}}$: log of the age and season-specific mean pseudo-growth rate,
- μ_W : mean log weight-at-age 0,
- $\sigma_{\log W_{obs}}$: observation error for log weight-at-age,
- $\mu_{W_{0,a}}$: initial mean log weight for each age.

The model includes random effects on both recruitment weight and growth, using a lognormal distribution:

$$\varepsilon_{G\,t,a} \sim N\left(0, \sigma_{\log \varepsilon_G}\right) \quad (23)$$

$$\varepsilon_{W_y} \sim N(0, \sigma_{\log \varepsilon_W}) \quad (24)$$

These capture inter-annual and seasonal variation not explained by fixed effects. They were modelled as random effects based on exploratory data analysis, which revealed substantial temporal variation in weight-at-age across years and seasons (see Supplementary Material 5).

The model is informed by mean weight-at-age data obtained from both the PELGAS and JUVENA scientific surveys, over a 15 year-period, from 2010 to 2024. PELGAS data were used to fit the model's predictions for odd-numbered time steps, while JUVENA data informed the predictions for even-numbered time steps. The observations were incorporated using a lognormal likelihood:

$$\log W_{t,a} \sim \mathrm{N}(\log \widehat{\mathrm{W}}_{\mathrm{t,a}}, \sigma_{\log W_{obs}}) \quad (25)$$

2.3. Maximum likelihood estimation through TMB

Model estimation was realized through Maximum Likelihood Estimation within the TMB package (Template Model Builder - Kristensen et al., 2016). TMB implements (1) Laplace approximation to evaluate the marginal likelihood, and Automatic Differentiation for fast computation of derivatives. Standard errors are computed through the delta method.

3. Results

3.1 Model checking and fit to data

Model convergence was assumed to have occurred if the absolute value of the final gradient of the marginal likelihood with respect to the fixed effects was <0.0001 for all parameters, and the Hessian matrix was positive definite. See the Supplementary Material 3 for full details on model validation and fit.

3.2 Comparing assessment model (SS3) and state space model (MY-PEL) estimates of key demographic parameters

Estimates of key demographic parameters (natural mortality, fishing mortality, spawning biomass and recruitment) produced by the state-space model MY-PEL were compared to those from the current assessment model, SS3. The results are illustrated in Figure 9.

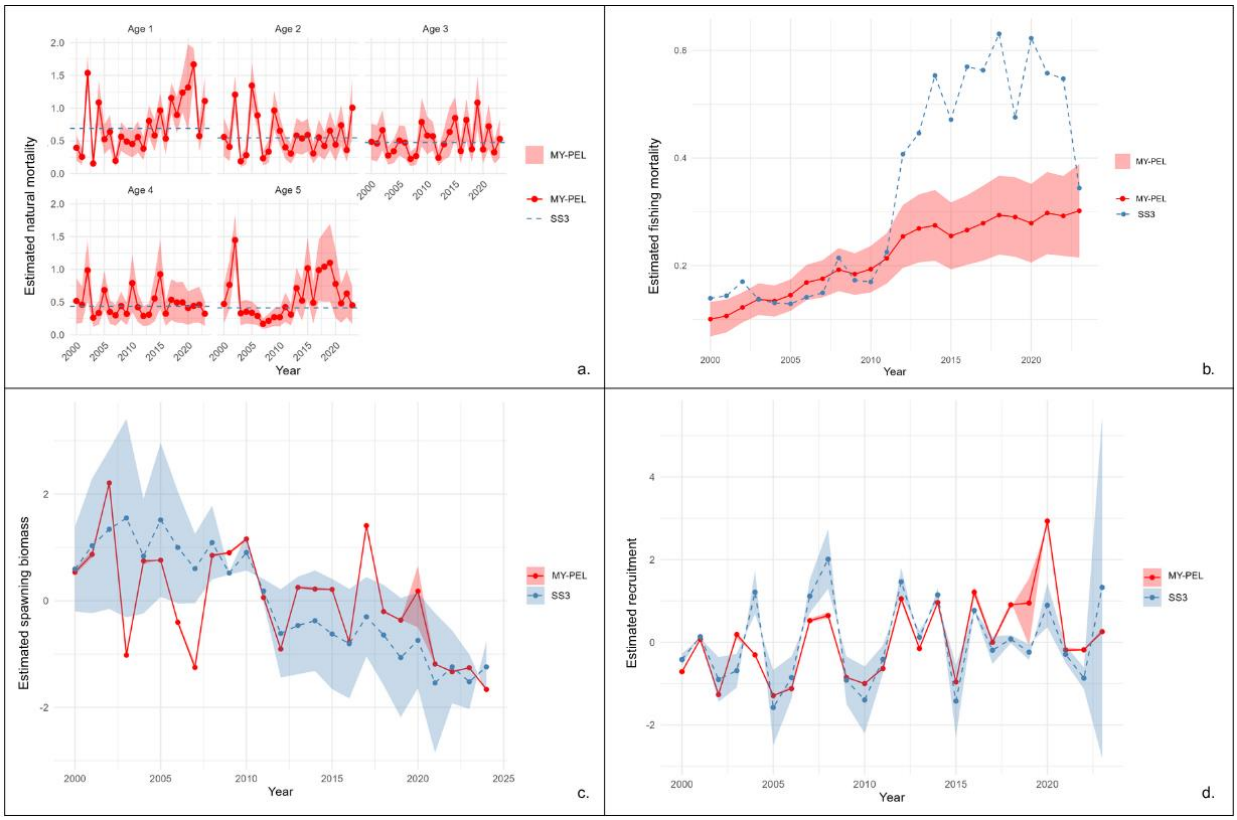

Fig. 9: Comparison between MY-PEL and SS3 demographic parameters estimates: a. Natural mortality, b. Fishing mortality, c. Spawning biomass (standardized), d. Recruitment (standardized)

Overall, MY-PEL and SS3 outputs show consistent trends: increasing fishing mortality, decreasing biomass and strong interannual variability in recruitment (Fig. 15, d). However, some discrepancies appear, especially for fishing mortality (Fig. 15, b). From 2011 onward, SS3 estimates show a stronger increase in fishing mortality, reaching values up to twice those produced by MY-PEL. The decline in spawning biomass (Fig. 15, c) also appears more pronounced in the SS3 outputs, while MY-PEL estimates display greater interannual fluctuations.

Regarding natural mortality (Fig. 15, a)., the temporal variability introduced in MY-PEL reveals both interannual fluctuations and apparent trends across age groups. For instance, natural mortality for age-1 individuals appears to increase steadily between 2012 and 2022, and similarly for age-6 individuals between 2010 and 2020 – patterns that cannot be captured by the SS3 model which assumes constant natural mortality over time.

3.3 [Q1] Does using data from a different season change our perception of the state of the stock?

3.3.1 Reconstruction of length-at-age, weight-at-age and abundances at age for autumn season

Since the JUVENA data were structured by length, an age–length key was applied to convert them into age-structured data, allowing their integration into the models. The procedure is detailed in section 2.1.1.c. It results in an age-length key (Fig. 10), the age composition for ages 1 to 6+ (Fig. 11), as well as a recruitment index (Fig. 12).

The resulting age-length key, illustrated in Figure 10, allows the estimation of the age composition from the length-structured JUVENA data, a critical step in integrating this survey in our age-structured state space models.

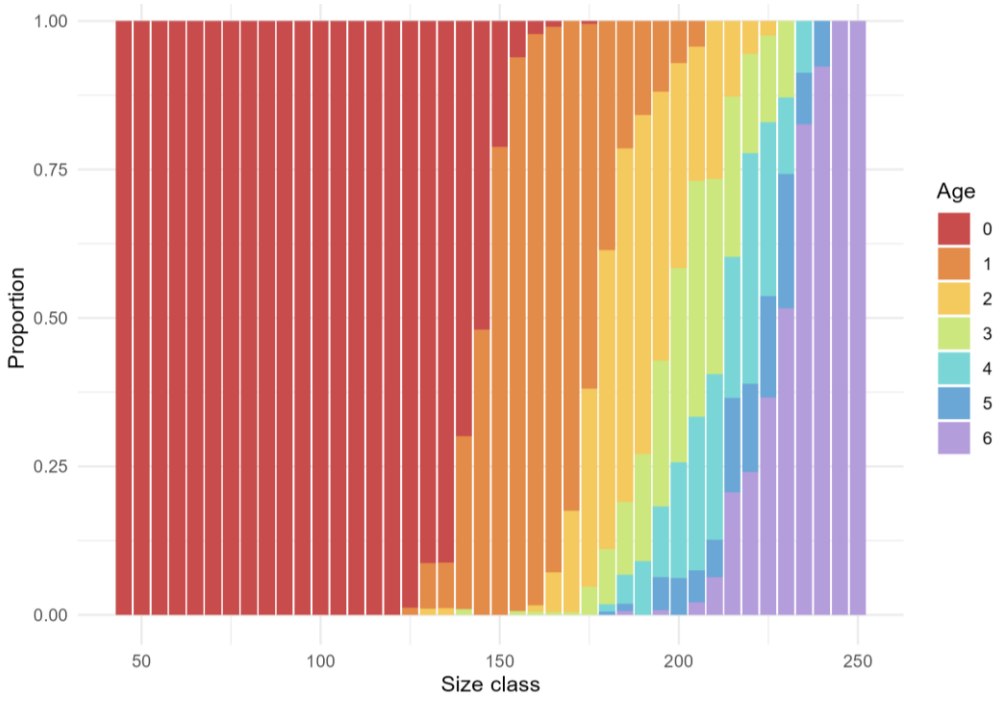

Fig. 10: Length-age key for fall constructed with the aggregation of EVHOE and fishery data

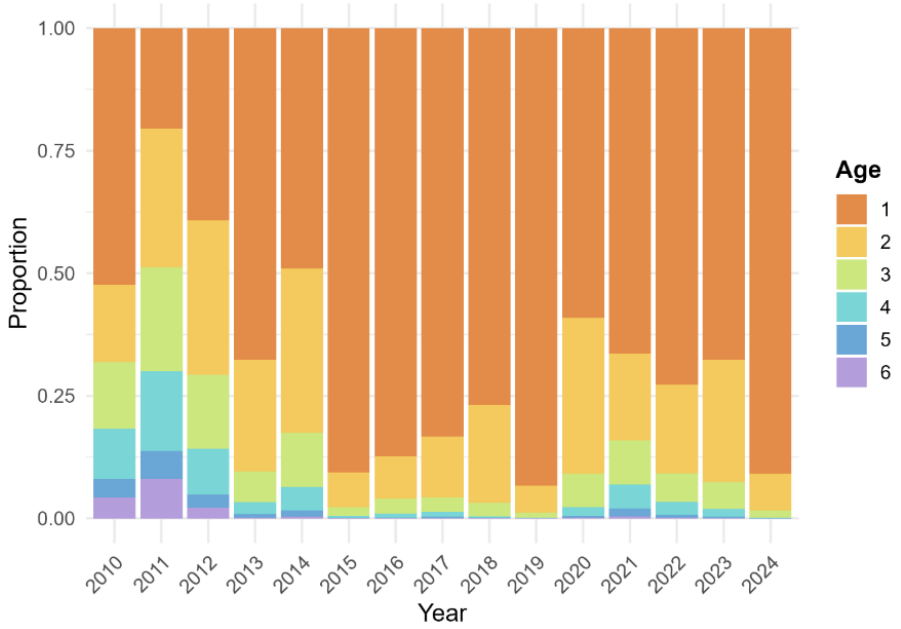

Fig. 11: Age composition data from the JUVENA survey informing abundance models

Like the PELGAS survey, the age composition from JUVENA shows a strong dominance of age-1 individuals, along with a clear decline in the proportion of age-4 and older fish over the past fifteen years. The proportion of these older age classes is even lower in the JUVENA data than in the PELGAS dataset.

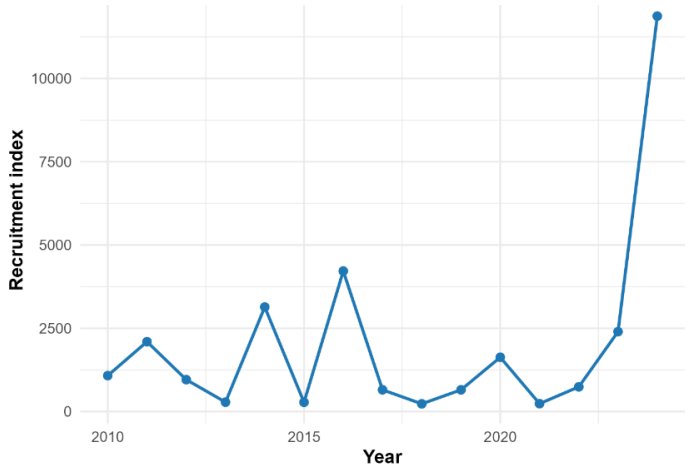

Fig. 12: Recruitment index data from the JUVENA survey informing abundance models

The recruitment index obtained from the JUVENA data displays strong interannual variability, with a very high value for 2024. The time series does not allow to see if such a high value has been observed before 2010.

3.3.2 Comparison of key demographic parameter estimates between a Spring-based (MY-PEL) and an Autumn-based (MY-JUV) model

Key demographic parameters estimated by two annual state-space models, one informed by Spring data (MY-PEL) and the other by Autumn data (MY-JUV) were compared. These results are presented in Figure 13.

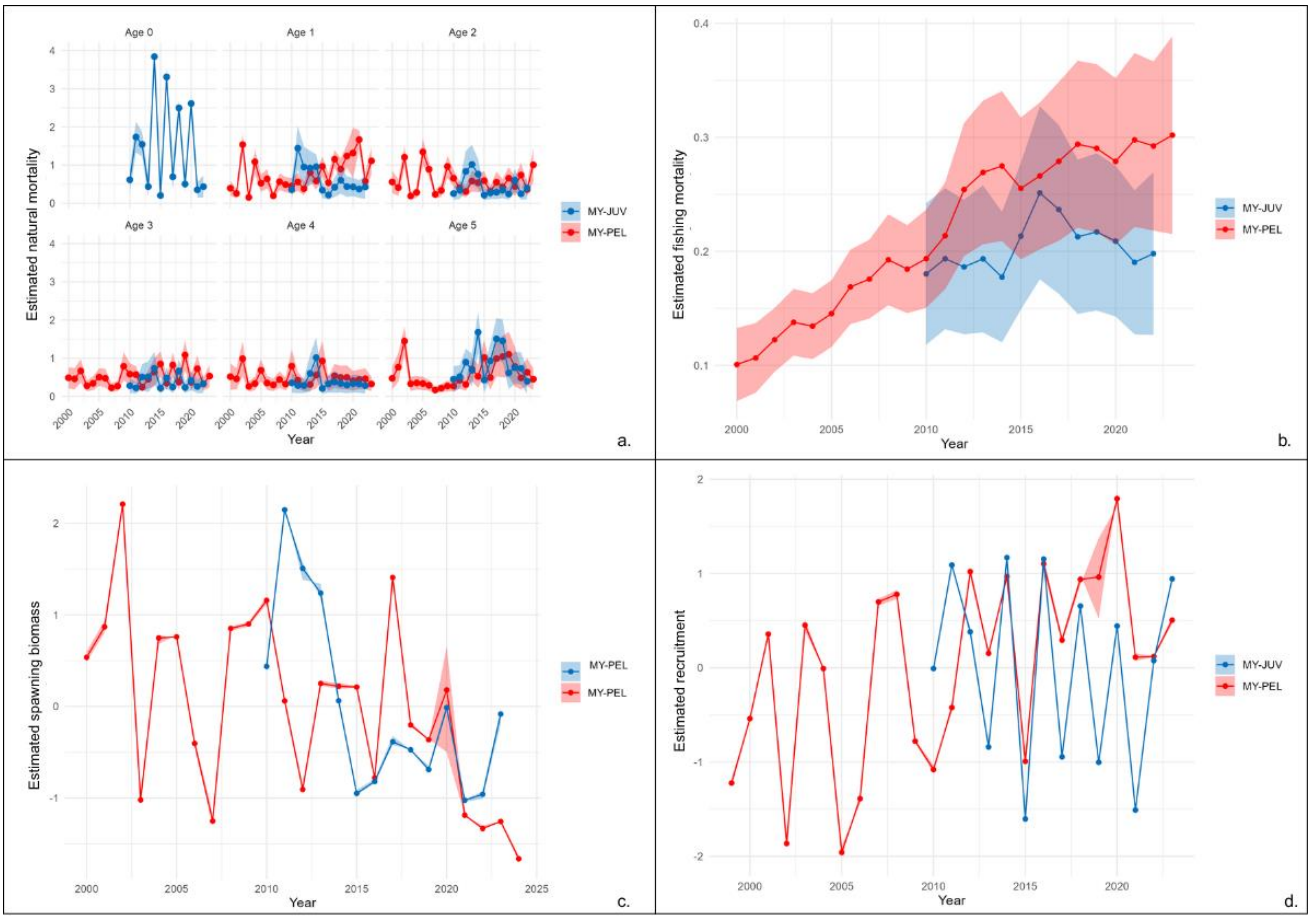

Fig. 13: Comparison between MY-PEL and MY-JUV demographic parameters estimates: a. Natural mortality, b. Fishing mortality, c. Spawning biomass (standardized), d. Recruitment (standardized)

Overall, using data from different seasons in annual state-space models leads to notable differences in the estimation of key demographic parameters. While both models estimate an increasing trend in fishing mortality (Fig. 13b), its overall magnitude is lower in MY-JUV. Natural mortality (Fig. 13a), and spawning biomass (Fig. 13c) estimates evolve within the same range of values for both models but exhibit very distinct, sometimes opposed, temporal patterns. The most striking concerns recruitment (Fig. 13d), which was defined differently in the two models: it is directly estimated for age-0 individuals with MY-JUV because the JUVENA survey focuses on juvenile fish, while with MY-PEL, recruitment corresponds to age-1 abundance of the following year. The MY-JUV estimates display stronger interannual variability, characterized by alternating periods of lower and higher values. This can be related to the strong age 0 natural mortality observed in Fig. 13a.

3.4 [Q2] Can we estimate seasonal varying growth and mortality for sardines in the Bay of Biscay? [Q3] Is growth higher during productive seasons and mortality higher during unproductive seasons?

The M-SEAS model enabled the estimation of both natural and fishing mortality on a seasonal time scale, while the G-SEAS model estimated growth over the same seasonal temporal resolution. The variability of these parameters in both models are shown in Figure 14.

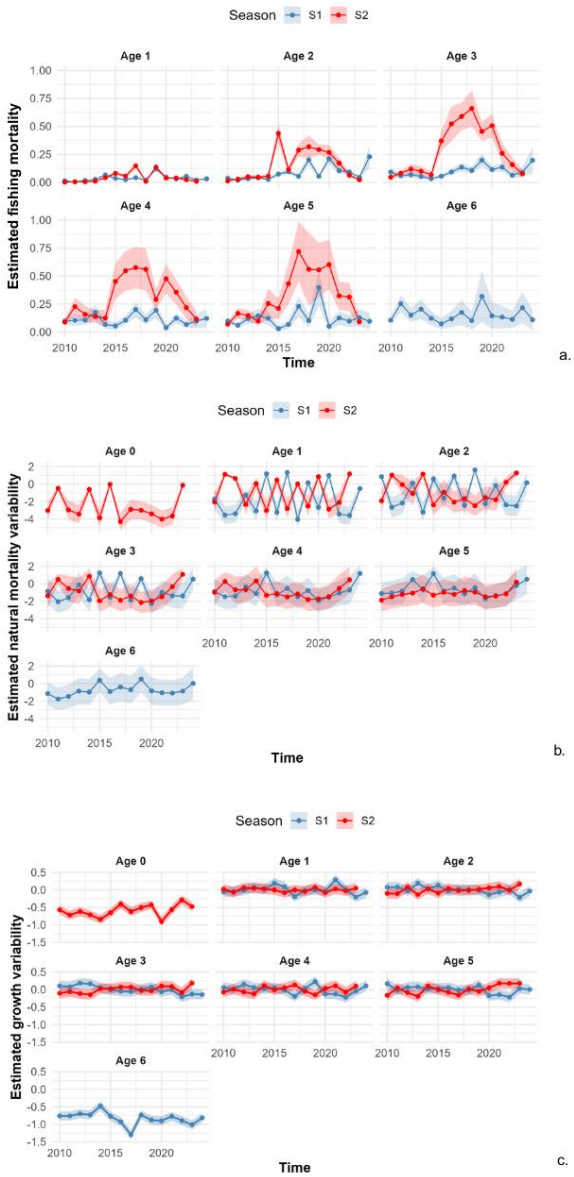

Fig. 14: Key demographic parameters variability estimates from the seasonal models M-SEAS and G-SEAS: a. Fishing mortality, b. Variability of natural mortality, c. Variability of growth

Two key patterns emerge from the fishing mortality estimates (Fig. 14a). First, fishing mortality is highest for individuals aged 3 to 5. Second, it is substantially higher during Season 2 compared to Season 1, although this seasonal difference is less pronounced for age-1 individuals.

Estimates of natural mortality variability (Fig. 14b) reveal contrasting trends between the two seasons, often exhibiting opposite patterns: when natural mortality is low in Season 1, it tends to be high in Season 2, and vice versa. This seasonal opposition is particularly pronounced for ages 1 and 2.

According to Figure 14c., growth estimates display lower overall variability, and show little to no difference between the two seasons.

Here, we focus not on the variability of these parameters, but on the temporal evolution of natural mortality and growth themselves, as shown in Figure 15.

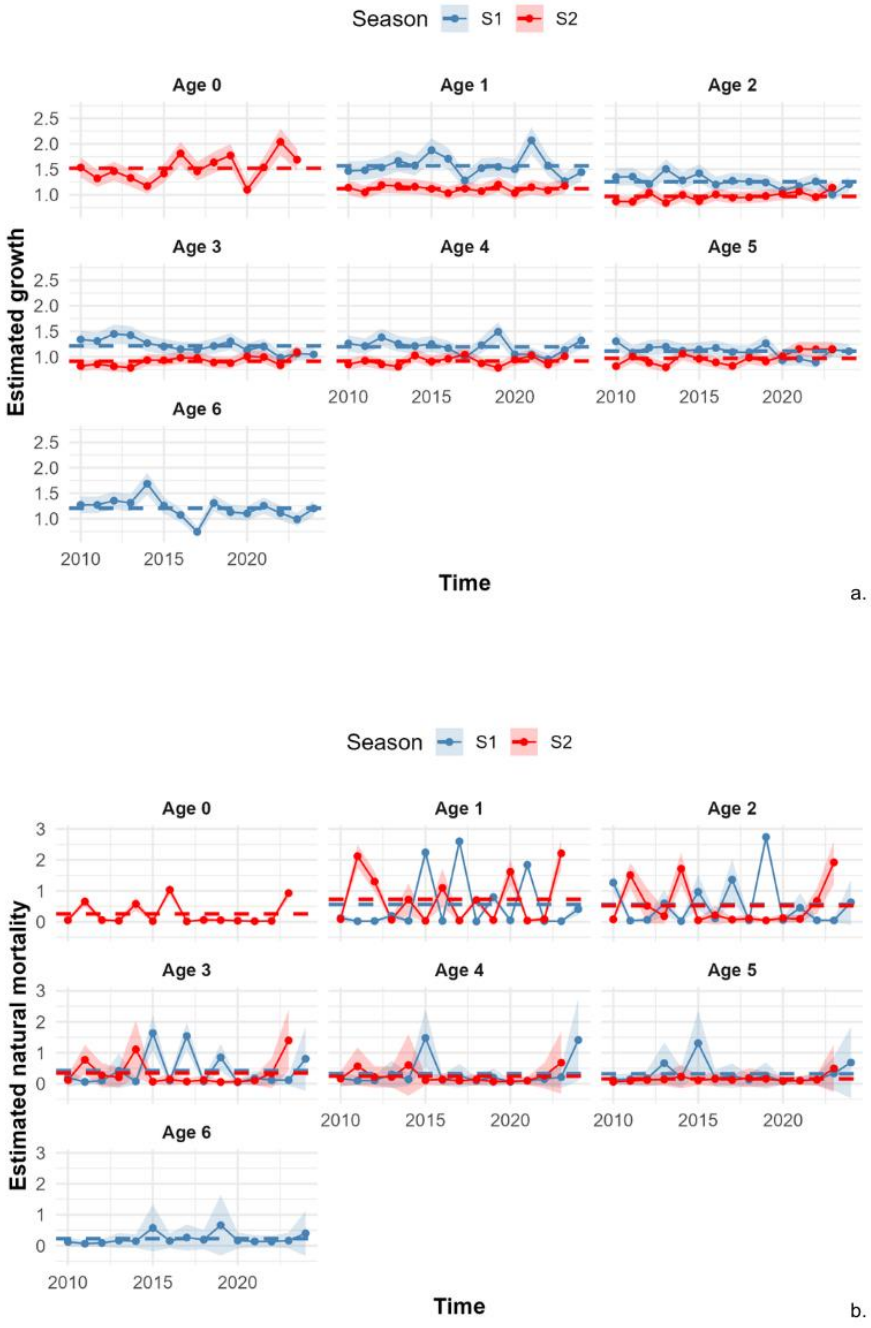

Fig. 15: Key demographic parameters estimates from the seasonal models M-SEAS and G-SEAS: a. Natural mortality, b. Growth. Dashed lines indicate the mean value for each age and season.

As previously observed, growth estimates by age and season remain relatively stable, with limited variability around the mean (Fig. 15a). As expected, growth values are higher in Season 1, both on average and across individual years, with seasonal differences decreasing with increasing age. Mean growth is also greater for younger individuals, especially at ages 0 and 1.

In contrast, mean natural mortality does not differ substantially between Season 1 and Season 2 (Fig. 15b), contrary to initial expectations. However, the alternating seasonal pattern described earlier—where low mortality in one season coincides with high mortality in the other—is once again apparent, particularly for ages 1 and 2.

3.5 [Q4] Is higher mortality during unproductive seasons preceded by low growth during the productive seasons?

To explore this question, we conducted a linear regression. It assessed the relationship between estimated natural mortality in Season 2 and estimated growth in Season 1 of the same year, and for the same age (Fig. 16).

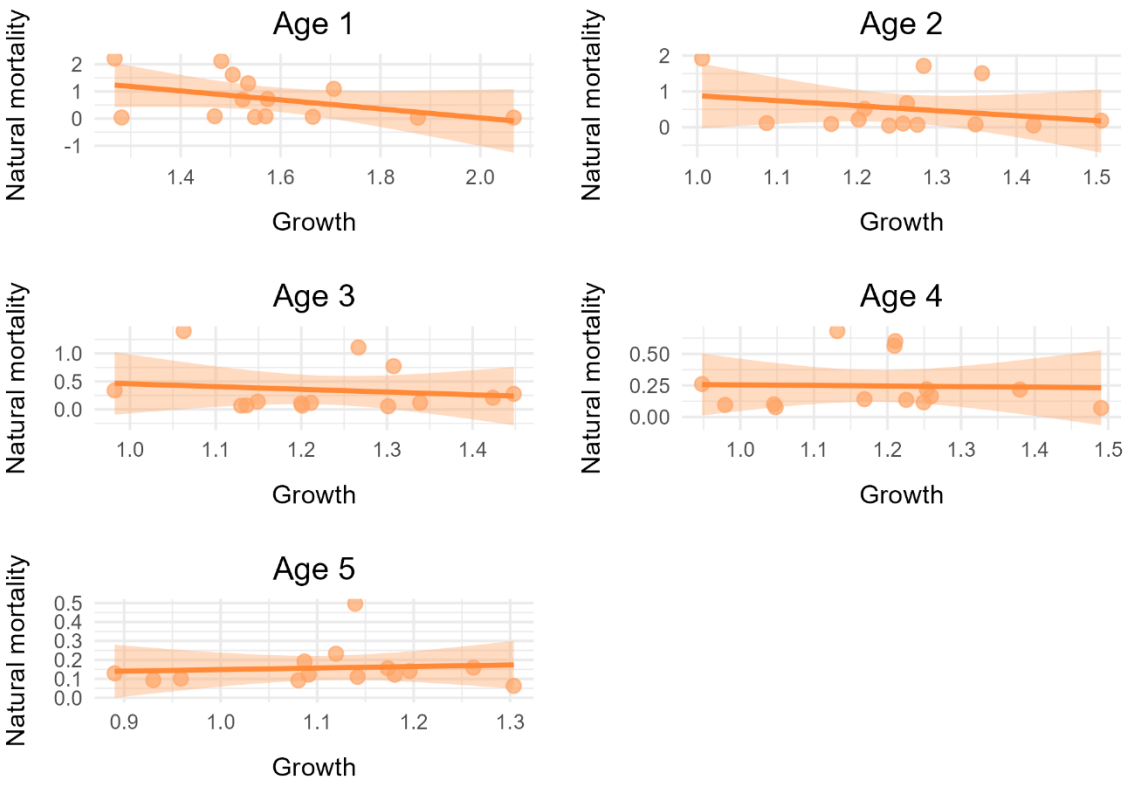

Fig. 16: Linear regressions between natural mortality during season 1 and growth during season 2 of the previous year, for each age class (ages 1 to 5). Each panel represents a separate age, with regression lines and 95% confidence intervals.

None of the regressions presented in Figure 16 provided statistically significant results. However, when examining the relationship between growth during the productive season (Season 1) and natural mortality in the following unproductive season (Season 2), a negative correlation can be observed for ages 1 and 2. No apparent correlation is observed for ages 3 to 5.

4. Discussion

This work introduced several methodological innovations, both in the yearly and seasonal models. First, natural mortality was treated as time-varying rather than stationary, as is typically assumed in assessment models (ICES and WGHANSA, 2024). This approach revealed strong interannual variability in natural mortality (MY-PEL).

Second, we used JUVENA age-0 abundance as a recruitment index, following the approach adopted for anchovy assessments. This choice allowed us to capture strong interannual variability in recruitment, which is characteristic of most pelagic fish species.

Third, models were developed on a seasonal temporal scale, explicitly estimating growth as a demographic rate and incorporating time-varying, age-dependent natural mortality. The introduction of a seasonal time step proved particularly important, as it revealed new insights into the intra-annual variability of sardine demographic rates. Specifically, our study revealed: seasonal differences in the variability of growth and natural mortality, higher growth during the first season (S1), especially at younger ages, alternating seasonal patterns in natural mortality, indicating potential density-dependence for ages 1 and 2, and age-specific relationships between successive seasons.

4.1 [Q1.1] Does using a state space model (MY-PEL) improve the assessment of sardines in the Bay of Biscay?

The MY-PEL model developed during this master thesis will contribute to the upcoming benchmark and may lead to changes in the assessment of sardine in the Bay of Biscay. Accounting for the temporal variability of natural mortality is particularly important to avoid bias in the estimation of key demographic parameters (Correa et al., 2023). Here, it allowed to see an increasing trend in natural mortality for both age-1 and age-6 sardines. While for age-1 sardines this observation is consistent with the data exploration (see Supplementary Material 5), for age-6 sardines it might rather represent a movement of older sardines towards northern regions (McKeown et al., 2025) than actual mortality.

In addition, MY-PEL introduced time-varying fishery selectivity by implementing age-specific random walks for fishing mortality. This further supports the growing body of literature demonstrating that state-space models are particularly well-suited for stock assessment (Auger-Méthé et al., 2021; Berg and Nielsen, 2016; Stock and Miller, 2021).

4.2 [Q1.2] Does using data from a different season change our perception of the state of the stock?

The use of JUVENA survey data is a novel aspect of this work and required data transformation before being integrated into the MY-JUV model. Since the JUVENA campaign targets juvenile fish, the resulting age-0 abundance index provides a more accurate proxy for recruitment. Applying this index as a recruitment indicator for sardine is innovative and offers a fresh perspective on recruitment dynamics in the Bay of Biscay. Furthermore, preliminary results from the PELGAS 2025 survey support the MY-JUV estimate of exceptionally high recruitment in 2024, reflected by a particularly large abundance of age-1 fish (Fig. 17).

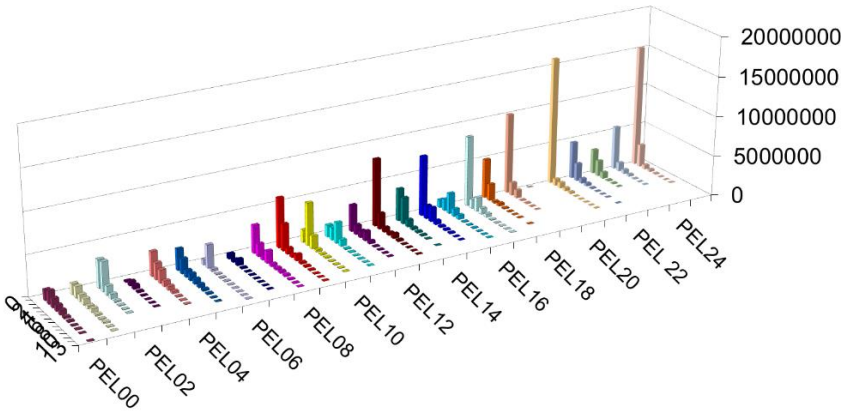

Fig. 17: Temporal evolution of the age composition of fish sampled during the PELGAS survey.

The difference in annual natural mortality estimates between the MY-PEL and MY-JUV models arises from the timing of the surveys. Because one occurs in spring and the other in autumn, each captures the population at a different stage of the annual cycle. The spring survey reflects survival after winter, when overwintering mortality, which is often high for juveniles, has already occurred. The autumn survey, in contrast, integrates mortality over the productive season, when food is generally abundant but other sources of mortality such as predation or density-dependent effects may occur. Depending on the year and environmental conditions, the two seasons may estimate very different values of natural mortality, especially for younger ages.

4.3 [Q2] Can we estimate seasonal varying growth and mortality for sardines in the Bay of Biscay?

Growth showed similar levels of variability in both seasons, with overall low variability over time, consistent with the findings of Bordes et al. (Under review). Detecting temporal variability in growth may require the use of standardized data rather than absolute values (Stawitz et al., 2015). Indeed, absolute growth values vary little in small pelagic fish because the steepest part of the von Bertalanffy growth curve occurs between age 0 and age 1. Nevertheless, obtaining an accurate representation of growth remains crucial in stock assessment to avoid biased perceptions of stock status (Stawitz and Essington, 2019).

In contrast, the results for natural mortality revealed variability across all ages and both seasons, with greater variability observed at younger ages (0–2). This could be explained by the higher sensitivity of younger sardines to environmental conditions.

4.4 [Q3] Are growth higher during productive seasons and mortality higher during unproductive seasons?

The results indicated higher growth during the productive season, consistent with the literature and largely explained by greater food availability (Gatti et al., 2018; Rosa et al., 2010). Growth was also higher for ages 0 and 1, in line with the von Bertalanffy growth model for sardines, which predicts higher growth rates at early life stages.

Mean natural mortality was similar across seasons, but opposite seasonal trends emerged, particularly for ages 1 and 2. This pattern suggests a density-dependent process (Myers and Cadigan, 1993): when survival is high in one season, mortality tends to increase in the next. Such dynamics are consistent with the findings of Bordes et al. (Under review), which revealed a strong density-dependence for age-1 natural mortality, although on a yearly scale. The stronger signal of density dependence at younger ages may be explained by their greater proportional abundance in the stock (see Fig. 4c, Fig. 11) and by their higher reliance on phytoplankton compared to older sardines, which have a more diversified diet (Bertrand et al., 2022).

The observed levels of natural mortality are difficult to interpret, as they may be confounded with survey catchability.

4.5 [Q4] Is higher mortality during unproductive seasons preceded by low growth during the productive seasons?

While it's important to keep in mind that no significant results were obtained from the linear regressions, some trends could be observed, that can be analyzed with caution. For ages 1 and 2, there seems to be a negative correlation). If the same trend was to become significant with more data collected, it would be coherent with overwintering, which is especially true for younger ages because the fish are smaller: reaching a threshold size is necessary to survive winter (Schultz and Conover, 1999, 1997; Van Deurs et al., 2011, 2010). No correlation was observed for older ages which can be explained by the fact that once the threshold size is reached, growth has no effect on survival during winter.

4.6 Limits

This work presents several limitations. First, the limited availability of JUVENA survey data required the use of EVHOE survey and fishery data, both of which are known to contain biases. In addition, EVHOE data were not weighted by spatial biomass, and only a single age–length key was used for all years, which does not account for temporal variability in the age–length relationship. Furthermore, JUVENA data are only available from 2010 onwards, which constrains the length of the time series that can be analysed with seasonal models.

The JUVENA recruitment index built in this work needs to be validated for sardine, as this survey mainly focuses on anchovy. This validation could be done by evaluating the potential bias of the index (spatial coverage, trawling strategy…), calculating the estimation error around this index and validating its capacity to distinguish interannual variability.

Growth was modelled using weight, but this approach may introduce bias: weight can fluctuate not only due to somatic growth but also because of physiological changes such as gonad development and shifts in energy reserves associated with reproduction, as shown by (Brosset et al., 2016). To obtain a more reliable estimate of growth independent of these confounding factors, tracking length instead of weight could be more appropriate.

4.7 Recommendations

To build upon the work presented in this paper, we recommend several methodological improvements. First, incorporating size-to-age structured data transformation within the model would

allow the propagation of uncertainty related to the data used to build the age-length key. Second, including a stock–recruitment relationship would enable the development of a full life-cycle model, more representative of ecological reality (Bordes et al, Under review). As observed, there appears to be a density-dependent effect at early ages in sardine, supported by the literature; this could be directly integrated into the model, with abundance influencing natural mortality and potentially growth, as in Bordes et al. (Under review). In addition, the explicit link between natural mortality and growth could also be incorporated, following the approach of Bordes et al. Extending the time series back to 2000, using the state-space framework to inform the missing years with the PELGAS data, would provide a better overview of population changes over the past two decades. Finally, integrating seasonal environmental data could offer further insight into the drivers of current changes in sardine population dynamics.

References

Allen, T.F., Hoekstra, T.W., Allen, T.F.H., 1992. Toward a unified ecology, Complexity in ecological systems series. Columbia Univ. Press, New York.

Auger-Méthé, M., Newman, K., Cole, D., Empacher, F., Gryba, R., King, A.A., Leos-Barajas, V., Mills Flemming, J., Nielsen, A., Petris, G., Thomas, L., 2021. A guide to state–space modeling of ecological time series. Ecological Monographs 91, e01470. https://doi.org/10.1002/ecm.1470

Bertrand, M., Brosset, P., Soudant, P., Lebigre, C., 2022. Spatial and ontogenetic variations in sardine feeding conditions in the Bay of Biscay through fatty acid composition. Marine Environmental Research 173, 105514. https://doi.org/10.1016/j.marenvres.2021.105514

Boëns, A., Grellier, P., Lebigre, C., Petitgas, P., 2021. Determinants of growth and selective mortality in anchovy and sardine in the Bay of Biscay. Fisheries Research 239, 105947. https://doi.org/10.1016/j.fishres.2021.105947

Bordes, A., Huret, M., Rivot, E., Andrieux, C., Edeline, E., Lebigre, C., Olmos, M., Under review. Disentangling the influence of density-dependence, size-dependence and environmental effects on fish population dynamics. Journal of Animal Ecology.

Boyra, G., Nogueira, E., Sobradillo, B., 2003. JUVENA survey. https://doi.org/10.57762/A6T5-9D32

Brosset, P., Lloret, J., Muñoz, M., Fauvel, C., Van Beveren, E., Marques, V., Fromentin, J.-M., Ménard, F., Saraux, C., 2016. Body reserves mediate trade-offs between life-history traits: new insights from small pelagic fish reproduction. Royal Society Open Science 3, 160202. https://doi.org/10.1098/rsos.160202

Cole, J., McGlade, J., 1998. Clupeoid Population Variability, the Environment and Satellite Imagery in Coastal Upwelling Systems. Reviews in Fish Biology and Fisheries 8, 445–471. https://doi.org/10.1023/A:1008861224731

Coombs, S.H., Smyth, T.J., Conway, D.V.P., Halliday, N.C., Bernal, M., Stratoudakis, Y., Alvarez, P., 2006. Spawning season and temperature relationships for sardine (*Sardina pilchardus*) in the eastern North Atlantic. J. Mar. Biol. Ass. 86, 1245–1252. https://doi.org/10.1017/S0025315406014251

Correa, G.M., Monnahan, C.C., Sullivan, J.Y., Thorson, J.T., Punt, A.E., 2023. Modelling time-varying growth in state-space stock assessments. ICES Journal of Marine Science 80, 2036–2049. https://doi.org/10.1093/icesjms/fsad133

Cury, P., Bakun, A., Crawford, R.J.M., Jarre, A., Quiñones, R.A., Shannon, L.J., Verheye, H.M., 2000. Small pelagics in upwelling systems: patterns of interaction and structural changes in “wasp-waist” ecosystems. ICES J Mar Sci 57, 603–618. https://doi.org/10.1006/jmsc.2000.0712

Doray M., Boyra, G., and van der Kooij, J. (Eds.) (2021) ICES Survey Protocols - Manual for acoustic surveys coordinated under ICES Working Group on Acoustic and Egg Surveys for Small Pelagic Fish (WGACEGG). 1st Marine Environmental Sciences Vol. 64. 100 pp. https://doi.org/10.17895/ices.pub.746

Doray, M., Petitgas, P., Romagnan, J.B., Huret, M., Duhamel, E., Dupuy, C., Spitz, J., Authier, M., Sanchez, F., Berger, L., Dorémus, G., Bourriau, P., Grellier, P., Massé, J., 2018. The PELGAS survey: Ship-based integrated monitoring of the Bay of Biscay pelagic ecosystem. Progress in Oceanography, Multidisciplinary integrated surveys 166, 15–29. https://doi.org/10.1016/j.pocean.2017.09.015

Gatti, P., Cominassi, L., Duhamel, E., Grellier, P., Le Delliou, H., Le Mestre, S., Petitgas, P., Rabiller, M., Spitz, J., Huret, M., 2018. Bioenergetic condition of anchovy and sardine in the Bay of Biscay and English Channel. Progress in Oceanography 166, 129–138. https://doi.org/10.1016/j.pocean.2017.12.006

Grandrémy, N., 2023. Dynamiques spatio-temporelles du zooplancton, en lien avec l’habitat et les petits poissons pélagiques, dans le Golfe de Gascogne. (phdthesis). Nantes Université.

ICES, 2024. Working Group on Southern Horse Mackerel, Anchovy and Sardine (WGHANSA). ICES Scientific Reports. https://doi.org/10.17895/ICES.PUB.23507922

ICES, WGHANSA, 2025. Working Group on Southern Horse Mackerel, Anchovy, and Sardine (WGHANSA). ICES Scientific Reports. https://doi.org/10.17895/ICES.PUB.29335520
ICES, WGHANSA, 2024. Working Group on Southern Horse Mackerel, Anchovy and Sardine (WGHANSA). ICES Scientific Reports. https://doi.org/10.17895/ICES.PUB.26003356
Koutsikopoulos, C., Le Cann, B., 1996. Physical processes and hydrological structures related to the Bay of Biscay anchovy. Scientia Marina.
Kristensen, K., Nielsen, A., Berg, C.W., Skaug, H., Bell, B.M., 2016. TMB: Automatic Differentiation and Laplace Approximation. Journal of Statistical Software 70, 1–21. https://doi.org/10.18637/jss.v070.i05
Levin, S.A., 1992. The Problem of Pattern and Scale in Ecology: The Robert H. MacArthur Award Lecture. Ecology 73, 1943–1967. https://doi.org/10.2307/1941447
Levin, S.A., Grenfell, B., Hastings, A., Perelson, A.S., 1997. Mathematical and Computational Challenges in Population Biology and Ecosystems Science. Science 275, 334–343. https://doi.org/10.1126/science.275.5298.334
Longhurst, A.R., 2010. Ecological Geography of the Sea. Elsevier.
McKeown, N.J., Lebigre, C., Van Der Kooij, J., Huret, M., 2025. Hierarchical Neutral and Non-Neutral Spatial Genetic Structuring in the European Sardine (*Sardina pilchardus*) Revealed by Genomic Analysis: Implications for Management. Evolutionary Applications 18, e70080. https://doi.org/10.1111/eva.70080
Menu, C., Pecquerie, L., Bacher, C., Doray, M., Hattab, T., van der Kooij, J., Huret, M., 2023. Testing the bottom-up hypothesis for the decline in size of anchovy and sardine across European waters through a bioenergetic modeling approach. Progress in Oceanography 210, 102943. https://doi.org/10.1016/j.pocean.2022.102943
Merritt, J.F., Lima, M., Bozinovic, F., 2001. Seasonal regulation in fluctuating small mammal populations: feedback structure and climate. Oikos 94, 505–514. https://doi.org/10.1034/j.1600-0706.2001.940312.x
Methot, R.D., Wetzel, C.R., 2013. Stock synthesis: A biological and statistical framework for fish stock assessment and fishery management. Fisheries Research 142, 86–99. https://doi.org/10.1016/j.fishres.2012.10.012
Myers, R.A., Cadigan, N.G., 1993. Density-Dependent Juvenile Mortality in Marine Demersal Fish. Can. J. Fish. Aquat. Sci. 50, 1576–1590. https://doi.org/10.1139/f93-179
Nielsen, A., Berg, C.W., 2014. Estimation of time-varying selectivity in stock assessments using state-space models. Fisheries Research, SI: Selectivity 158, 96–101. https://doi.org/10.1016/j.fishres.2014.01.014
Ogle, D.H., Doll, J.C., Wheeler, A.P., Dinno, A., 2015. FSA: Simple Fisheries Stock Assessment Methods. https://doi.org/10.32614/CRAN.package.FSA
Olmos, M., Ianelli, J., Ciannelli, L., Spies, I., McGilliard, C.R., Thorson, J.T., 2023. Estimating climate-driven phenology shifts and survey availability using fishery-dependent data. Progress in Oceanography 215, 103035. https://doi.org/10.1016/j.pocean.2023.103035
Rockwell, S.M., Wunderle, J.M., Sillett, T.S., Bocetti, C.I., Ewert, D.N., Currie, D., White, J.D., Marra, P.P., 2017. Seasonal survival estimation for a long-distance migratory bird and the influence of winter precipitation. Oecologia 183, 715–726. https://doi.org/10.1007/s00442-016-3788-x
Rosa, R., Gonzalez, L., Broitman, B., Garrido, S., Santos, A., Nunes, M., 2010. Bioenergetics of small pelagic fishes in upwelling systems: relationship between fish condition, coastal ecosystem dynamics and fisheries. Mar. Ecol. Prog. Ser. 410, 205–218. https://doi.org/10.3354/meps08635
Schaub, M., Abadi, F., 2011. Integrated population models: a novel analysis framework for deeper insights into population dynamics. Journal of Ornithology 152, 227–237. https://doi.org/10.1007/s10336-010-0632-7
Schultz, E.T., Conover, D.O., 1999. The allometry of energy reserve depletion: test of a mechanism for size-dependent winter mortality. Oecologia 119, 474–483. https://doi.org/10.1007/s004420050810

Schultz, E.T., Conover, D.O., 1997. Latitudinal differences in somatic energy storage: adaptive responses to seasonality in an estuarine fish (Atherinidae: Menidia menidia). Oecologia 109, 516–529. https://doi.org/10.1007/s004420050112

Simmonds, E.J., MacLennan, D.N., MacLennan, D.N., 2005. Fisheries acoustics: theory and practice, 2nd ed. ed, Fish and aquatic resources series. Blackwell Science, Oxford ; Ames, Iowa.

Stawitz, C.C., Essington, T.E., 2019. Somatic growth contributes to population variation in marine fishes. Journal of Animal Ecology 88, 315–329. https://doi.org/10.1111/1365-2656.12921

Stawitz, C.C., Essington, T.E., Branch, T.A., Haltuch, M.A., Hollowed, A.B., Spencer, P.D., 2015. A state-space approach for detecting growth variation and application to North Pacific groundfish. Can. J. Fish. Aquat. Sci. 72, 1316–1328. https://doi.org/10.1139/cjfas-2014-0558

Stock, B.C., Miller, T.J., 2021. The Woods Hole Assessment Model (WHAM): A general state-space assessment framework that incorporates time- and age-varying processes via random effects and links to environmental covariates. Fisheries Research 240, 105967. https://doi.org/10.1016/j.fishres.2021.105967

Stratoudakis, Y., Coombs, S., De Lanzós, A.L., Halliday, N., Costas, G., Caneco, B., Franco, C., Conway, D., Santos, M.B., Silva, A., Bernal, M., 2007. Sardine (Sardina pilchardus) spawning seasonality in European waters of the northeast Atlantic. Mar Biol 152, 201–212. https://doi.org/10.1007/s00227-007-0674-4

Van De Wolfshaar, K.E., De Roos, A.M., Persson, L., 2008. POPULATION FEEDBACK AFTER SUCCESSFUL INVASION LEADS TO ECOLOGICAL SUICIDE IN SEASONAL ENVIRONMENTS. Ecology 89, 259–268. https://doi.org/10.1890/06-2058.1

Van Deurs, M., Christensen, A., Frisk, C., Mosegaard, H., 2010. Overwintering strategy of sandeel ecotypes from an energy/predation trade-off perspective. Mar. Ecol. Prog. Ser. 416, 201–214. https://doi.org/10.3354/meps08763

Van Deurs, M., Hartvig, M., Steffensen, J.F., 2011. Critical threshold size for overwintering sandeels (Ammodytes marinus). Mar Biol 158, 2755–2764. https://doi.org/10.1007/s00227-011-1774-8

Varpe, Ø., 2017. Life History Adaptations to Seasonality. Integrative and Comparative Biology 57, 943–960. https://doi.org/10.1093/icb/icx123

Véron, M., Duhamel, E., Bertignac, M., Pawlowski, L., Huret, M., 2020. Major changes in sardine growth and body condition in the Bay of Biscay between 2003 and 2016: Temporal trends and drivers. Progress in Oceanography 182, 102274. https://doi.org/10.1016/j.pocean.2020.102274

https://doi.org/10.1016/j.pocean.2020.102274

Vert-pre, K.A., Amoroso, R.O., Jensen, O.P., Hilborn, R., 2013. Frequency and intensity of productivity regime shifts in marine fish stocks. Proceedings of the National Academy of Sciences 110, 1779–1784. https://doi.org/10.1073/pnas.1214879110

White, E.R., Hastings, A., 2020. Seasonality in ecology: Progress and prospects in theory. Ecological Complexity 44, 100867. https://doi.org/10.1016/j.ecocom.2020.100867

Williams, C.M., Ragland, G.J., Betini, G., Buckley, L.B., Cheviron, Z.A., Donohue, K., Hereford, J., Humphries, M.M., Lisovski, S., Marshall, K.E., Schmidt, P.S., Sheldon, K.S., Varpe, Ø., Visser, M.E., 2017. Understanding Evolutionary Impacts of Seasonality: An Introduction to the Symposium. Integrative and Comparative Biology 57, 921–933. https://doi.org/10.1093/icb/icx122

Appendices (Supplementary Material)

Appendix 1 – Using EVHOE and fishery data

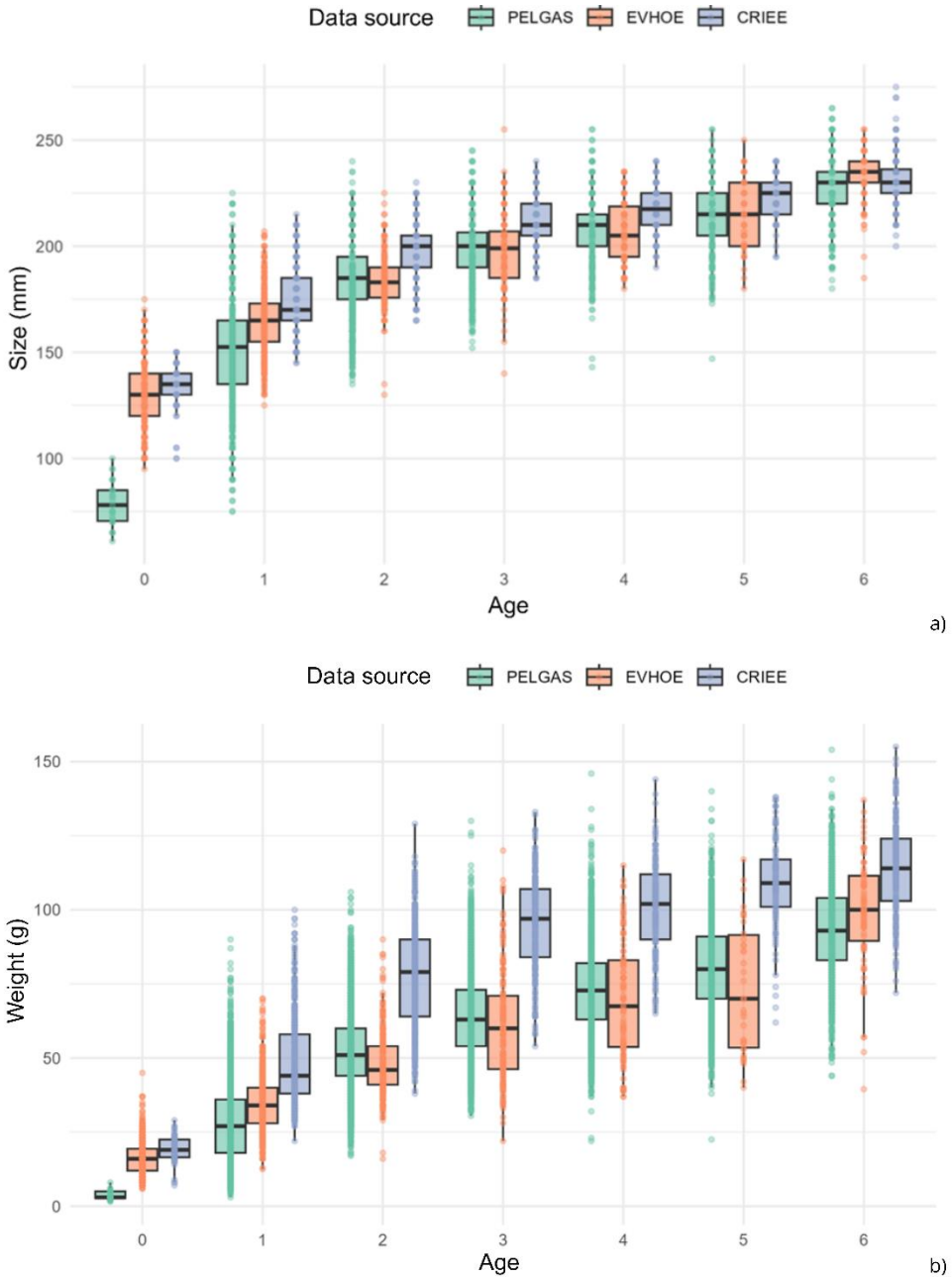

Fig. 18: Age-length relationship (a) and age-weight relationship (b) for different data sources.

The age–length and age-weight relationships presented in Fig. 18 show that from age 2 onwards, the mean size and weight for EVHOE is lower than for PELGAS, while the mean size and weight for the fishery (CRIEE) is higher. Since EVHOE takes place after PELGAS, it is not biologically plausible for fish to be smaller at that later time. This discrepancy can be explained by survey selectivity: EVHOE is a bottom-trawl survey, which is not designed to target small pelagic fish and may therefore sample smaller individuals than PELGAS. In contrast, the fishery data are biased because fishermen preferentially target larger, higher-value fish. To compensate for the lack of data from JUVENA, we therefore used the mean of EVHOE and fishery values, considering that one underestimates and the other overestimates fish size.

Appendix 2 – MY-PEL model

Let $N_{t,a}$ denote the estimated abundance at age *a* (ranging from 1 to 6+) and time step *t* (ranging from 1 to 25, i.e the number of years between 2000 and 2024.

For ages 2 to 6+, log abundance was calculated recursively as the log abundance for previous age and previous year stage minus corresponding natural and fishing mortality.:

$$\log \widehat{N_{t+1,a+1}} = \begin{cases} \log \widehat{N_{t,a}} - M_{t,a} - F_{t,a} & if\ 2 \le a \le 5 \\ \log \widehat{N_{t,a+1}} - \log M_{t,a} - F_{t,a} + \log \widehat{N_{t,a}} - M_{t,a} - F_{t,a} & if\ a = 6 \end{cases} \quad (26)$$

At the initial time step t=1, the model is initialized for ages 1 to 6+:

$$\log \widehat{N_{1,a}} = \mu_{N_{0,a}} \qquad age\ a = 1, \dots, 6 \quad (27)$$

Recruitment is assumed to occur at age 1. The abundance of recruits was modelled with a year-specific random effect:

$$\log \widehat{N_{t,1}} = \mu_R + \varepsilon_{R\,t} \quad (28)$$

The natural mortality rate was modelled using a log-linear formulation:

$$\log M_{t,a} = \log \mu_{M_a} + \varepsilon_{M\,t,a} \quad (29)$$

Again, estimated index of abundance and spawning biomass at age were calculated from the estimated log abundance for ages 1 to 6+:

$$\widehat{I_{t,a}} = \widehat{N_{t,a}} * s_a * q \quad (30)$$

$$\widehat{I_{w_{t,a}}} = \widehat{N_{t,a}} * s_a * q * W_{t,a} \quad (31)$$

$$\widehat{SB_{t,a}} = \widehat{N_{t,a}} * mat_{t,a} * W_{t,a} \quad (32)$$

Where s_a corresponds to the survey selectivity for age *a*.

Total index of abundance and spawning biomass were then obtained by summing the age-specific values over ages 1 to 6:

$$\widehat{I_t} = \sum_{a=1}^{6} \widehat{I_{t,a}} \qquad (in\ number\ of\ fish) \quad (33)$$

$$\widehat{I_{w_t}} = \sum_{a=1}^{6} \widehat{I_{w_{t,a}}} \qquad (in\ biomass) \quad (34)$$

$$\widehat{SB_t} = \sum_{a=1}^{6} \widehat{SB_{t,a}} \quad (35)$$

The estimated catches in number of fish were calculated using a Baranov equation:

$$\widehat{C_{t,a}} = \frac{F_{t,a}}{F_{t,a}+M_{t,a}} * N_{t,a} * (1 - e^{-M_{t,a}-F_{t,a}}) \quad (36)$$

And converted into biomass using weight-at-age data from the fisheries:

$$\widehat{C_{w_{t,a}}} = C_{t,a} * W_{f_{t,a}} \quad (37)$$

Fishing selectivity at age *a* for year *t* was calculated as the fishing mortality at age *a* for year *t* divided by the total fishing mortality in that year:

$$s_{fishery_{t,a}} = \frac{F_{t,a}}{F_t} \quad (38)$$

In this model, the following were estimated as fixed effect parameters:

- q : catchability of the PELGAS survey
- q_{JUV} : catchability of the JUVENA survey,
- μ_R : mean log abundance at age 1,
- $\mu_{N_{0,a}}$: initial log abundance for each age.

And the following were fixed to a given value based on expertise:

- $\log \mu_{M_a}$: log of the age-specific mean natural mortality rate,
- $\sigma_{\log C_{obs}}$: observation error for catches,
- θ: Dirichlet parameter for the survey age composition,
- θ_F: Dirichlet parameter for the catches age composition.

The model includes random effects on recruitment abundance, natural and fishing mortality using a lognormal distribution for recruitment abundance and natural mortality:

$$\varepsilon_{M\,t,a} \sim N\left(0, \sigma_{\log \varepsilon_M}\right) \quad (39)$$

$$\varepsilon_{R\,t} \sim N(0, \sigma_{\log \varepsilon_W}) \quad (40)$$

And a random walk for fishing mortality:

$$\log F_{t,a} \sim \begin{cases} N(0,1), & t = 1 \\ N\left(\log F_{t-1,a}, \sigma_{\log \varepsilon_{F_a}}\right), & t > 1 \end{cases} \quad (41)$$

These capture inter-annual variation not explained by fixed effects. The use of a random walk for each age allows to implicitly estimate time varying selectivity (Nielsen and Berg, 2014).

The model is informed by yearly index of abundance and age composition (i.e., proportion of each age for a given year, calculated by dividing number at age by total number of fish) obtained from scientific surveys, and yearly catch and age composition for the fisheries.

The observations were incorporated using a lognormal likelihood or a Dirichlet:

Table 3: Likelihoods for the MY-PEL model

Notation	Data type	Unit	Likelihood
C_t	Seasonal fisheries catch	Tons	$\log C_t \sim N(\log \hat{C}_t, \sigma_{\log C}{}^2)$
I_t	Seasonal index of abundance	Number of fish	$\log I_t \sim N(\log \hat{I}_t, \sigma_{\log I}{}^2)$
$p_{AC_{t,a}}$	Age composition for the survey	Proportion	$p_{AC_{t,a}} \sim \text{Dirichlet}(\theta \cdot \widehat{p_{AC_{t,a}}})$
$p_{AC\_F_{t,a}}$	Age composition for the fisheries	Proportion	$p_{AC\_F_{t,a}} \sim \text{Dirichlet}(\theta_F \cdot \widehat{p_{AC\_F_{t,a}}})$

Appendix 3 – Model checking and fit to data

All models presented in this paper successfully converged, as indicated by the absolute value of the final gradient of the marginal likelihood with respect to the fixed effects being <0.0001 for all parameters, and by the Hessian matrix being positive definite. Model validation also considered goodness-of-fit, which is presented below.

MY-PEL

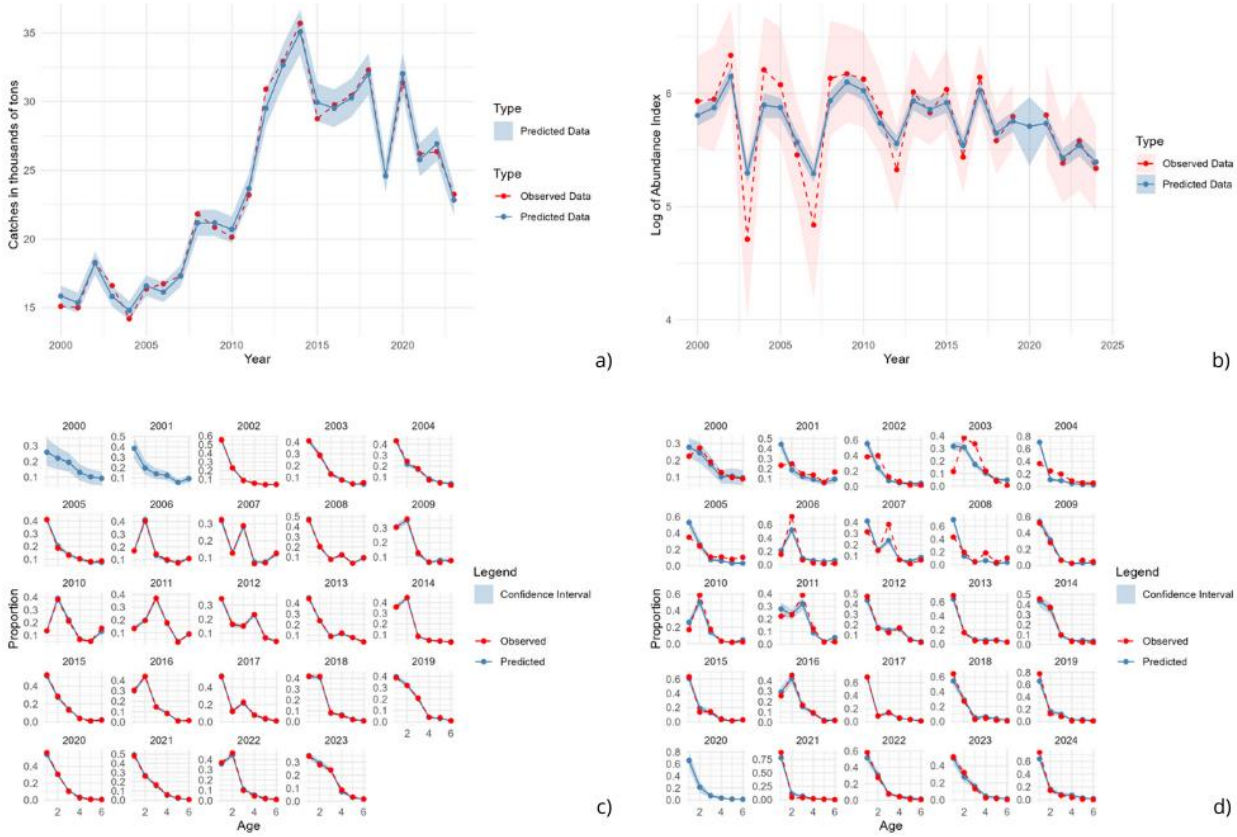

Fig. 19: Fit to data for the MY-PEL model.a. Catches. b. Abundance Index. c. Catches age composition. d. Survey age composition.

MY-JUV

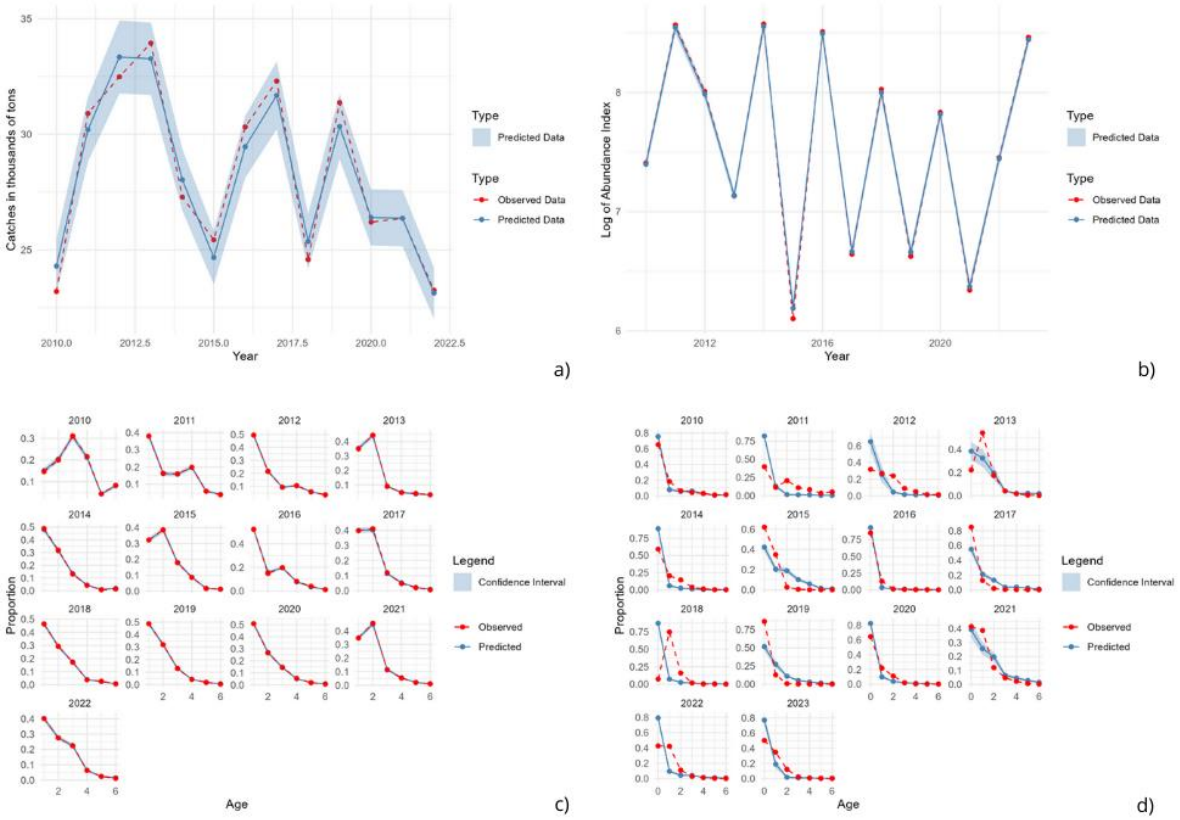

Fig. 20: Fit to data for the MY-JUV model.a. Catches. b. Abundance Index. c. Catches age composition. d. Survey age composition.

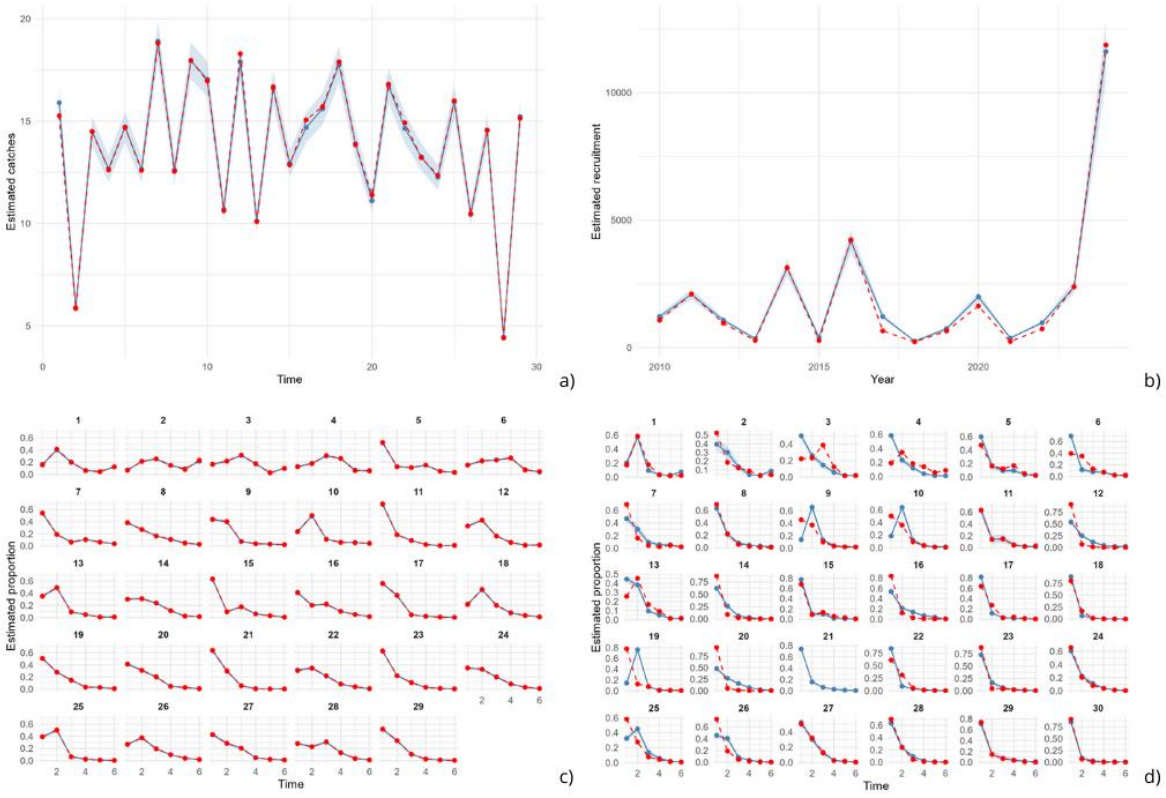

Fig. 21: Fit to data for the M-SEAS model. a. Catches. b. Recruitment Index. c. Catches age composition. d. Survey age composition.

Appendix 4 – Other predefined parameters entering the models (maturity and survey selectivity)

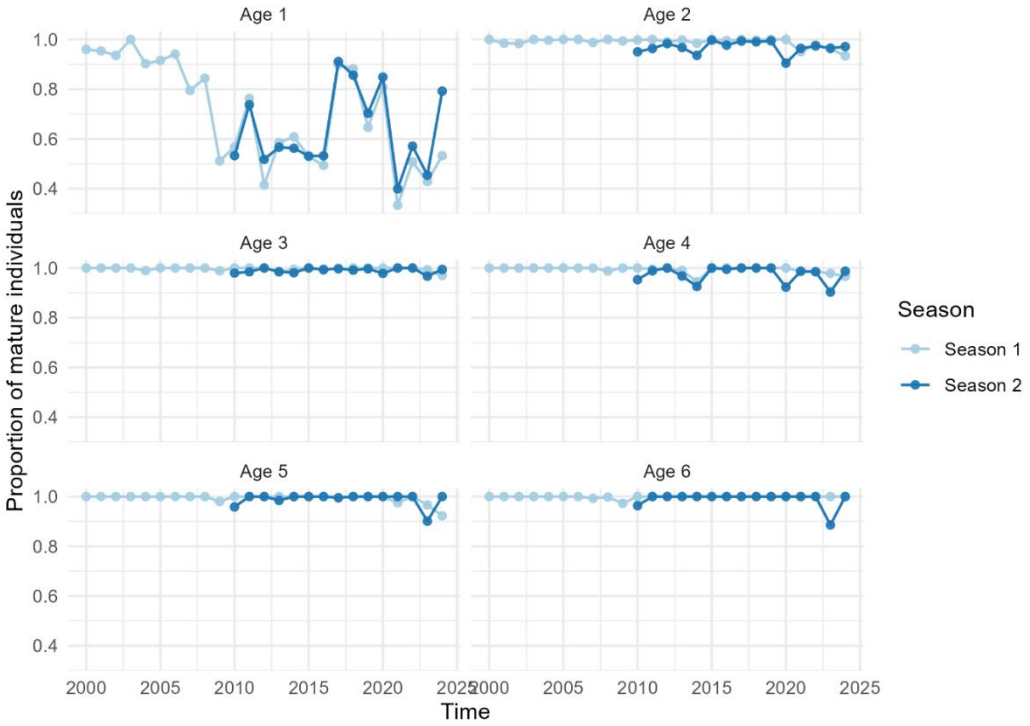

Fig. 22: Maturity data from the PELGAS survey (season 1) and the aggregation of EVHOE and fishery data (season 2)

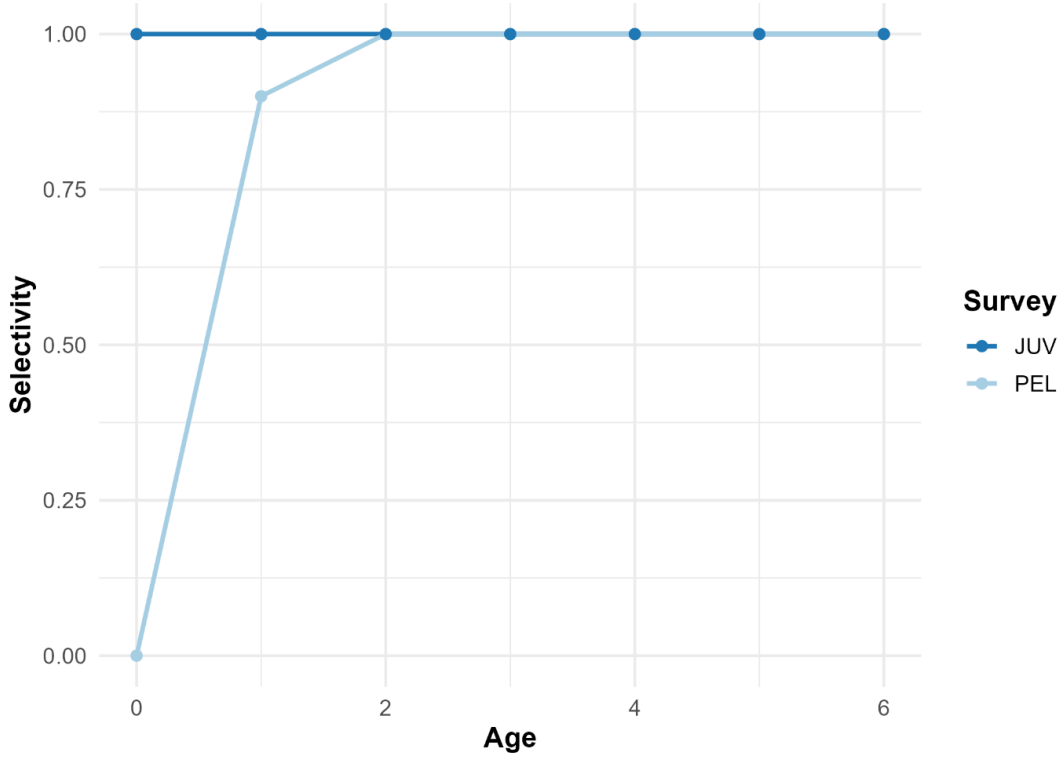

Fig. 23: Selectivity-at-age for the JUVENA and PELGAS surveys

Appendix 5 – Data exploration

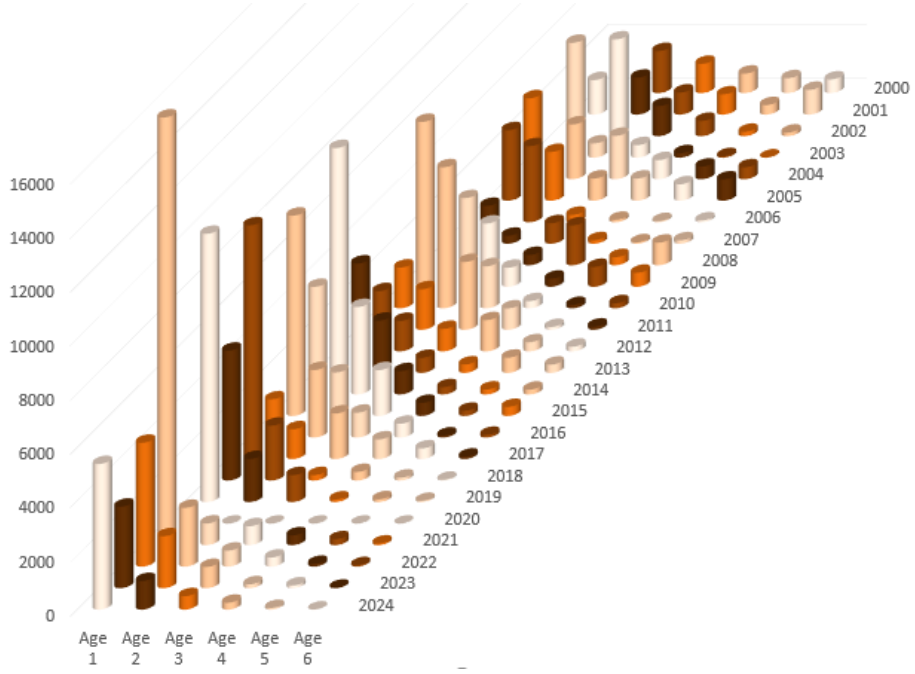

Fig. 24: Evolution of PELGAS age composition over time

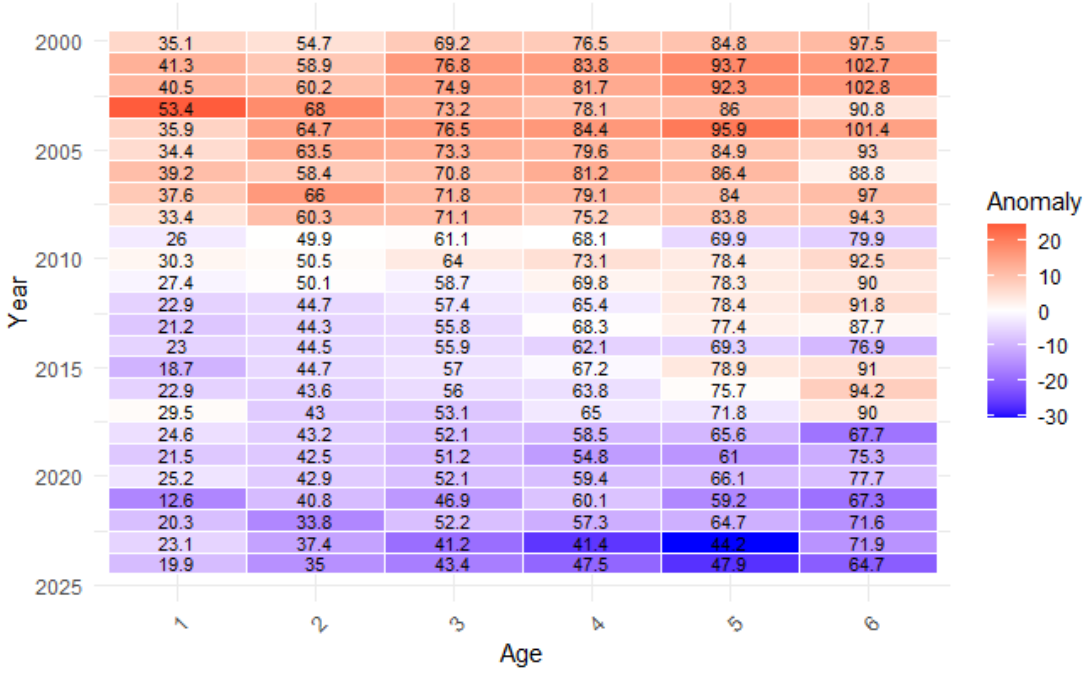

Fig. 25: Evolution of PELGAS weight-at-age anomaly (the numbers represent the mean weights-at-age)

Some preliminary data exploration was conducted before constructing the models, allowing us to examine trends in demographic parameters over the time period covered by the PELGAS data. The most striking trends were the increasing mortality of age-1 individuals (Fig. 24) and the marked decrease in weight-at-age (Fig. 25). These patterns highlight the importance of explicitly modelling time-varying growth and natural mortality.

Appendix 6 – Comparing My-PEL and SS3 stock assessment model

Natural mortality, fishing mortality, spawning biomass and recruitment estimates were not the only MY-PEL results compared to the SS3 stock assessment model and presented to WGHANSA. Here is available the comparison of the goodness-of-fit to data of both models.

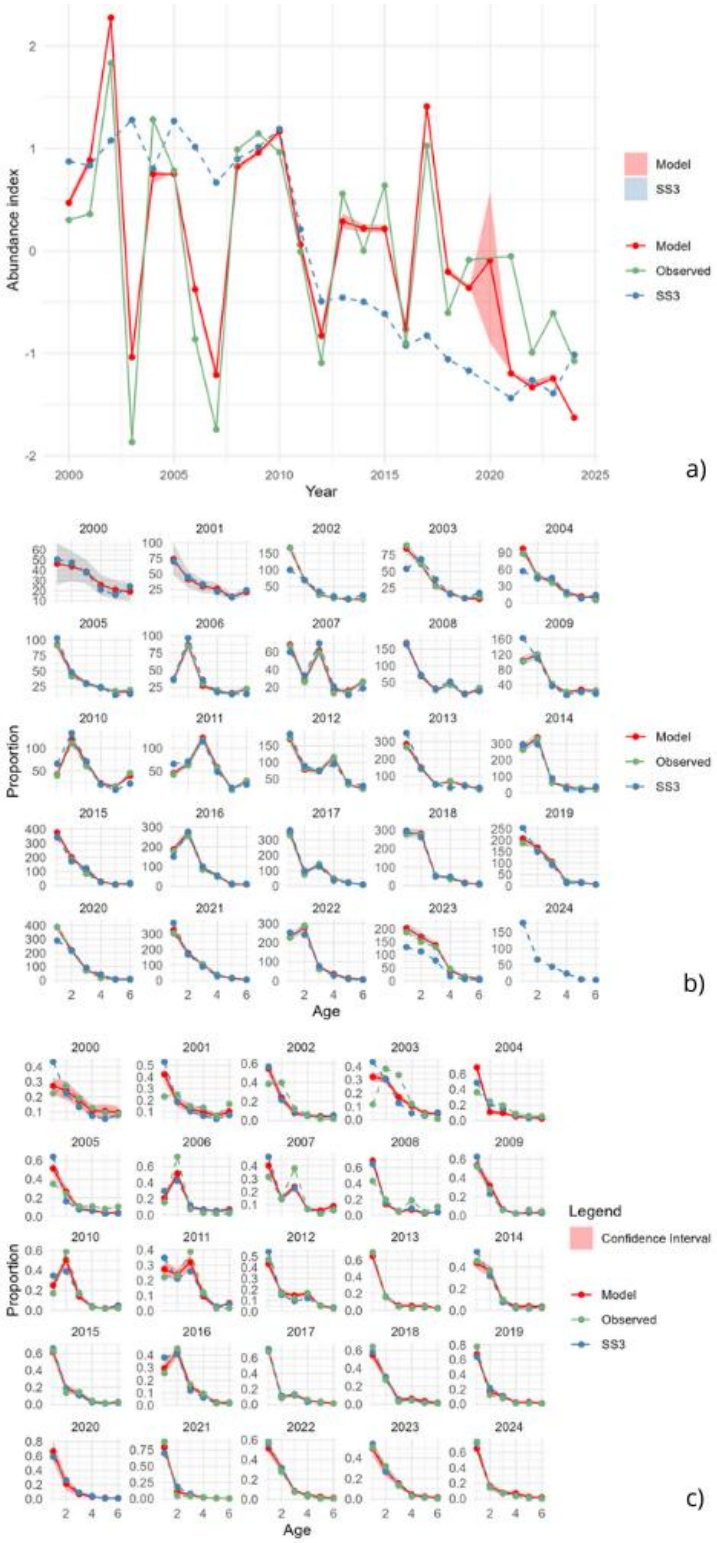

Fig. 26: Fit to data for My-PEL and SS3 stock assessment model. a. abundance index. b. Catches age composition. c. Survey age composition.

L'INSTITUT agro Rennes Angers	Diplôme : Ingénieur Spécialité : Ingénieur agronome Spécialisation / option : Sciences Halieutiques et Aquacoles / Ecologie Halieutique Enseignant référent : Pablo Brosset

Auteur(s) : Mila Déru Date de naissance* : 09/12/2003	Organisme d'accueil : Ifremer, LBH/HALGO Adresse : Centre Ifremer Bretagne ZI Pointe du Diable 29280 PLOUZANÉ Maître de stage : Maxime Olmos
Nb pages : 29 Annexe(s) : 6	
Année de soutenance : 2025	

Titre français : Comprendre la variabilité interannuelle des processus démographiques de la sardine dans le golfe de Gascogne : un modèle de dynamique de population saisonnier

Titre anglais : A seasonal population dynamics model to understand intra-annual variability in sardine demographic processes in the Bay of Biscay

Résumé (1600 caractères maximum) : Les sardines sont une espèce à courte durée de vie, avec des transitions rapides entre stades de vie et une forte variabilité saisonnière des processus démographiques comme la croissance et la mortalité. Dans le golfe de Gascogne, elles présentent depuis vingt ans un déclin de la taille, de la condition physique et de la survie. Les modèles actuels supposent pourtant une mortalité constante et une croissance fixe, et analysent la population à l'échelle annuelle, masquant la variabilité intra-annuelle. Ce stage vise à modéliser cette dynamique à une échelle saisonnière via un modèle à espace d'état et une inférence par TMB pour estimer croissance et mortalité selon la saison. Deux périodes ont été définies : la saison productive (avril–septembre), appuyée par les données PELGAS, et la saison moins productive (octobre–mars), basée sur JUVENA. Des modèles saisonniers intégrant plusieurs sources de données ont été développés pour étudier l'impact de la saisonnalité et évaluer si cette approche améliore la compréhension des changements récents. Les résultats montrent une meilleure croissance en saison productive, surtout chez les jeunes individus, tandis que la mortalité naturelle varie selon la saison, suggérant des mécanismes densité-dépendants. Ces travaux soulignent l'intérêt d'une approche saisonnière pour améliorer la gestion des stocks et mieux comprendre les facteurs environnementaux et démographiques influençant la sardine dans le golfe de Gascogne.

Abstract (1600 caractères maximum) : Sardines are a short-lived species, characterized by rapid transitions between life stages and strong seasonal variability in demographic processes such as growth and mortality. In the Bay of Biscay, they have experienced a decline in size, body condition, and survival over the past twenty years. Current models, however, assume constant mortality and fixed growth, and analyze the population at an annual scale, which masks intra-annual variability. This internship aims to model sardine population dynamics at a seasonal scale using a state-space model and TMB-based inference to estimate seasonal growth and mortality. Two periods were defined: the productive season (April–September), informed by PELGAS data, and the less productive season (October–March), based on JUVENA data. Seasonal models integrating multiple data sources were developed to study the impact of seasonality and to assess whether this approach improves understanding of recent population changes. Results show higher growth during the productive season, particularly in young individuals, while natural mortality varies across seasons, suggesting density-dependent mechanisms. These findings highlight the importance of a seasonal approach to improve stock management and better understand the environmental and demographic factors influencing sardines in the Bay of Biscay.

Mots-clés : Sardine, Dynamique de populations, Saisonnalité, Croissance, Mortalité, Modèle à espace d'état, Golfe de Gascogne

Key Words: Sardine, Population dynamics, Seasonality, Growth, Mortality, State-space model, Bay of Biscay